AD_____

Award Number: W81XWH-07-1-0250

TITLE: Development of Augmented Leukemia/Lymphoma-Specific T-Cell Immunotherapy for Deployment with Haploidentical, Hematompoietic Progenitor-Cell Transplant

PRINCIPAL INVESTIGATOR: Laurence Cooper, M.D., Ph.D.
Rita Young, Ph.D.

CONTRACTING ORGANIZATION: The University of Texas
MD Anderson Cancer Center
Houston, TX 77030

REPORT DATE: May 2008

TYPE OF REPORT: Annual

PREPARED FOR: U.S. Army Medical Research and Materiel Command
Fort Detrick, Maryland 21702-5012

REPORT DOCUMENTATION PAGE

Form Approved
OMB No. 0704-0188

1. REPORT DATE	2. REPORT TYPE	3. DATES COVERED
01-05-2008	Annual	15 Apr 2007 – 14 Apr 2008

4. TITLE AND SUBTITLE

Development of Augmented Leukemia/Lymphoma-Specific T-Cell Immunotherapy for Deployment with Haploidentical, Hematompoietic Progenitor-Cell Transplant

5a. CONTRACT NUMBER

5b. GRANT NUMBER
W81XWH-07-1-0250

5c. PROGRAM ELEMENT NUMBER

6. AUTHOR(S)

Laurence Cooper, M.D., Ph.D., Rita Young, Ph.D.

E-Mail: ljncooper@mdanderson.org

5d. PROJECT NUMBER

5e. TASK NUMBER

5f. WORK UNIT NUMBER

7. PERFORMING ORGANIZATION NAME(S) AND ADDRESS(ES)

The University of Texas
MD Anderson Cancer Center
Houston, TX 77030

8. PERFORMING ORGANIZATION REPORT NUMBER

9. SPONSORING / MONITORING AGENCY NAME(S) AND ADDRESS(ES)
U.S. Army Medical Research and Materiel Command
Fort Detrick, Maryland 21702-5012

10. SPONSOR/MONITOR'S ACRONYM(S)

11. SPONSOR/MONITOR'S REPORT NUMBER(S)

12. DISTRIBUTION / AVAILABILITY STATEMENT
Approved for Public Release; Distribution Unlimited

13. SUPPLEMENTARY NOTES

14. ABSTRACT
To develop T-cell therapies for B-cell malignancies we have developed a chimeric antigen receptor (CAR) which when expressed on the cell surface redirects T-cell specificity for CD19, a B-lineage cell-surface antigen. We have undertaken a series of systematic experiments to improve the ability of these CAR+ T cells to persist after adoptive transfer based on conditional expression of interleukin-2 (IL-2) which is a potent cytokine that can prolong T-cell persistence. Firstly, we have combined T-cell therapy with antibody therapy directing both immunotherapies to B-cell antigens. To improve CD19-specific T-cell survival we combined a CD20-specific antibody with IL-2 which deposits IL-2 in the tumor microenvironment and is a surrogate for T-cell help (TH). Secondly, we have developed a gene transfer platform to propagate CD19-specific CAR+ CD4+ T cells that provide TH to CD8+ T cells. Thirdly, we have re-engineered the CD19-specific CAR itself so that it can signal for endogenous production of IL-2 through chimeric CD28. These technologies will now be evaluated in animal models in preparation for deciding which to take forward to a clinical trial.

15. SUBJECT TERMS
Leukemia, Lymphoma, Transplant, Transplantation: bone marrow and stem cell, T-Cell Immunotherapy

16. SECURITY CLASSIFICATION OF:			17. LIMITATION OF ABSTRACT	18. NUMBER OF PAGES	19a. NAME OF RESPONSIBLE PERSON
a. REPORT	b. ABSTRACT	c. THIS PAGE			USAMRMC
U	U	U	UU	33	19b. TELEPHONE NUMBER *(include area code)*

Table of Contents

Page

INTEROFFICE MEMORANDUM

TO: US DEPARTMENT OF DEFENSE

FROM: LAURENCE COOPER[1]

CC: LESLIE LOPEZ[2]

DATE: 5/19/2008

SUBJECT: ANNUAL REPORT FOR DOD GRANT – INTRODUCTION

Department: Pediatrics - Patient Care
Agency: US Department of Defense
Sponsor Number: W91ZSQ6289N610
Award Number: W81XWH-07-1-0250 01
Project Period: 04/15/2007- 05/15/2011
Title: Development of Augmented Leukemia/Lymphoma-Specific T-Cell Immunotherapy for Deployment with Haploidentical Hematopoietic Progenitor-Cell Transplant

Human CD19-specific T cells, based on 1st-generation technology, are currently in a "first in human" clinical trial (BB-IND 11411, author L.J.N. Cooper). This proposal is currently optimizing the immunobiology of CD19-specific T cells to improve therapeutic potential by comparing three methods to improve the *in vivo* persistence and anti-tumor effect of infused T cells which have been genetically modified to be CD19-specific. At the end of this award period it will be known if these three approaches have the potential for improving therapeutic effect and this will lead to a 2nd-generation clinical trial after haploidentical hematopoietic progenitor-cell transplant (HPCT).

[1] ljncooper@mdanderson.org
[2] leslopez@mdanderson.org

INTEROFFICE MEMORANDUM

TO: US DEPARTMENT OF DEFENSE

FROM: LAURENCE COOPER[1]

CC: LESLIE LOPEZ[2]

DATE: 5/19/2008

SUBJECT: ANNUAL REPORT FOR DOD GRANT

Department: Pediatrics - Patient Care
Agency: US Department of Defense
Sponsor Number: W91ZSQ6289N610
Award Number: W81XWH-07-1-0250 01
Project Period: 04/15/2007- 05/15/2011
Title: Development of Augmented Leukemia/Lymphoma-Specific T-Cell Immunotherapy for Deployment with Haploidentical Hematopoietic Progenitor-Cell Transplant

ATTACHMENTS

(i) Papers:
   a. Cancer Res. 2007
   b. Cancer Res. 2008

(ii) Memo regarding feedback from Advisory Committee and Transition Planning

OVERVIEW

In this first year of this grant award we have made considerable progress to achieving the specific aims (tasks) identified in the application.

Task #1: Can CD10-specific-IL2 immunocytokine in combination with CD19-specific T cells improve persistence of infused T cells and to treat B-lineage malignancy?

The initial data for this aim has been published Cancer Res. 2007 Mar 15;67(6):2872-80 (as attached). These data demonstrate that a CD20-specific immunocytokine can augment the persistence and therapeutic effect of CD19-specific T cells. At this time we will not be generating a CD10-specific immunocytokine since addition approaches to providing T-cell help and improving persistence appear more promising (tasks #2 and #3).

Task #2: Can CD19-specific $CD4^+$ T_h cells improve the anti-tumor response of CD19-specific CD8+ T cells?

The initial data for this aim has been published Cancer Res. 2008 Apr 15;68(8):2961-71.0 (as attached). These data demonstrate that both $CD4^+$ and $CD8^+$ T cells expressing CD19-specific chimeric antigen receptor (CAR) can be generated using a novel non-viral gene transfer approach employing the *Sleeping Beauty* (*SB*) transposon/transposase system.

[1] ljncooper@mdanderson.org
[2] leslopez@mdanderson.org

In future experiments we will be undertaking an analysis of how the $CD4^+$ CAR^+ T cells contribute to the persistence of $CD8^+$ CAR^+ T cells and visa versa.

Task #3: Can CD28 co-stimulation can enhance the survival and potency of CD19-specific T cells?

Data (Figure 1 and Figure 2) indicates that second generation CAR (designated CD19RCD28) expressing CD28 endodomains provides a CD19-dependent fully-competent activation signal resulting in improved persistence (as measured by detection of T-cell fire fly luciferase, ffLuc) after adoptive transfer and augmented elimination of an established B-lineage malignancy, compared with 1st generation technology (designated CD19, which signals only through chimeric CD3ζ.

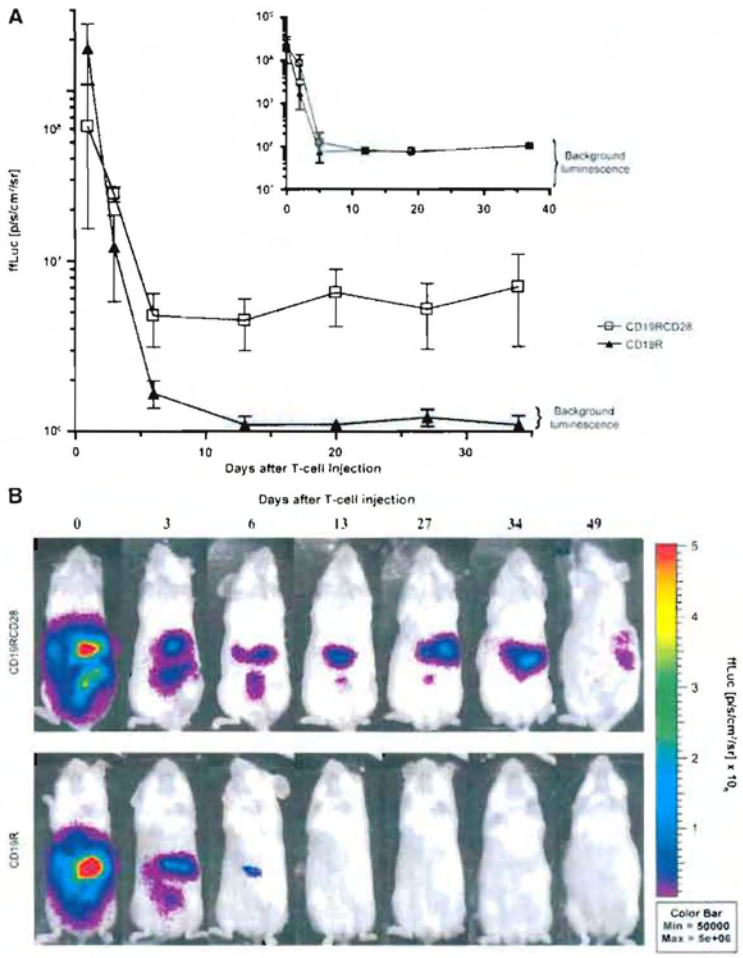

Figure 1: *In vivo* persistence of CAR^+ T cells. A, longitudinal monitoring of the bioluminescent signals of $5x10^6$ $ffLuc^+$ $CD19RCD28^+$ or $CD19R^+$ T cells injected into groups of four NOD/*scid* mice bearing $CD19^+$ Daudi tumor cells. Initial T-cell signal was measured 3 hours after injection. Points, mean photon flux (units $p/s/cm^2/sr$); bars, SD. Gray area, average background ffLuc-derived flux for a group of mice that did not receive injections of tumor or T cells. Inset, T-cell survival after adoptive transfer in NOD/*scid* mice that did not receive tumor. B, Pseudocolor image representing light intensity and anatomic localization of the ffLuc-derived T-cell signal in two representative mice. The color bar displays the ffLuc activity in $p/s/cm^2/sr$.

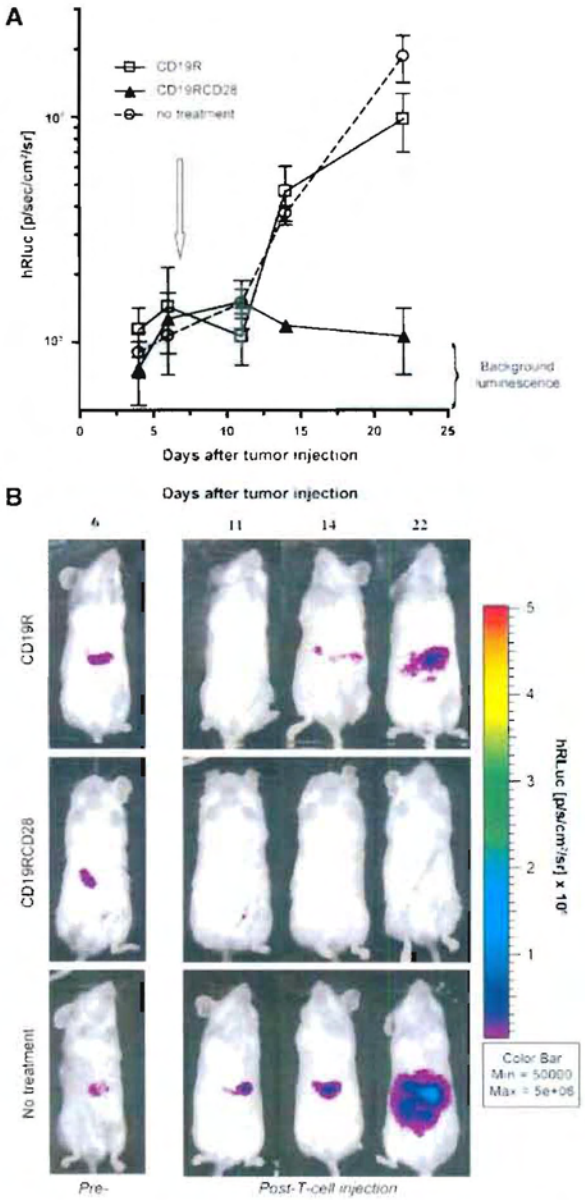

Figure 2: *In vivo* antitumor activity of CAR$^+$ T cells. A, longitudinal monitoring of the bioluminescent signals of hRluc$^+$ (Renilla luciferase) Daudi cells in NOD/*scid* mice. Mice with progressively growing tumors were separated into three groups (four mice per group) bearing comparable tumor loads. Seven days later (arrow), the mice were injected with $2x10^7$ ffLuc$^+$ CD19R$^+$ or CD19RCD28$^+$ T cells. A control group received no T-cell treatment. Points, mean photon flux (in p/s/cm2/sr); bars, SD. Using the Wilcoxon rank sum test, we detected a statistically significant difference between groups treated with CD19RCD28+ T cells and the control group ($P < 0.05$), no statistically significant difference between the groups receiving CD19R+ T cells and no treatment ($P > 0.05$). Gray area, average background hRluc-derived flux for a group of mice that did not receive injections of tumor or T cells. B, Pseudocolor image representing light intensity and anatomic localization of the hRluc-derived Daudi flux signals in three representative mice. The color bar displays the relative hRluc activity in p/s/cm2/sr.

TRANSITION TO CLINICAL TRIAL

We have significantly reduced the time to develop clinically-significant numbers of T cells genetically modified to be specific for CD19. One of the major hurdles to applying CAR^+ T cell and gene therapy technology to treat B-ALL has been the lengthy *ex vivo* manufacturing time to generate and release clinical-grade CD19-specific T cells, during which the pace of the underlying leukemic disease often prevents patients from receiving adoptive immunotherapy. Typically, it has required up to 100 days genetically modifying and propagating CAR^+ T cells to clinically-meaningful numbers, using non-viral (electroporation) gene transfer in compliance with current good manufacturing practices (cGMP). We have evaluated a new approach to reducing the time to therapy using Nucleofection (Amaxa), *SB* transposition and expanding of CAR^+ T cells on artificial antigen presenting cells.

To reduce immunogenicity, we are generating a codon-optimized (CoOp) humanized CD19-specific CAR, designated hCD19RCD28, where murine hypervariable or complementarity determining regions in CD19R have been replaced using sequences of humanized CD19-specific antibodies which are currently in the public domain. The hCD19RCD28 CAR will be expressed from a *SB* transposon DNA plasmid expressing hCD19RCD28. To improve safety by eliminating the potential for sustained expression of the *SB* transposase from insertion of DNA plasmid, we will electro-transfer non-integrating mRNA coding for *SB* transposase prepared by *in vitro* transcription, along with *SB* DNA transposon.

We are developing a new adoptive therapy trial to infuse *SB*-modified CD19-specific donor-derived T cells in patients with $CD19^+$ B-ALL after autologous hematopoietic stem cell transplantation (HSCT). An application has been sent to NIH-OBA for governmental review regarding the *SB* DNA plasmid vector containing CD19RCD28 transposon. Clinical-grade DNA *SB* transposon are being generated by Qiagen. Clinical-grade K562 aAPC are being prepared by PACT under auspices of NHLBI. The trial is under review by CRC. The IND is being written.

INTEROFFICE MEMORANDUM

TO: US DEPARTMENT OF DEFENSE

FROM: LAURENCE COOPER[1]

CC: LESLIE LOPEZ[2]

DATE: 5/19/2008

SUBJECT: ANNUAL REPORT FOR DOD GRANT: FEEDBACK FROM ADVISORY COMMITTEE AND TRANSITION PLANNING

Department: Pediatrics - Patient Care
Agency: US Department of Defense
Sponsor Number: W91ZSQ6289N610
Award Number: W81XWH-07-1-0250 01
Project Period: 04/15/2007- 05/15/2011
Title: Development of Augmented Leukemia/Lymphoma-Specific T-Cell Immunotherapy for Deployment with Haploidentical Hematopoietic Progenitor-Cell Transplant

On 05/06/2008 the advisory board was contacted and asked to score my progress per Section 6 "Supporting Documentation" of the original grant application. The members of the committee are:
1) Dr. Champlin, Professor, Chair, Blood & Marrow Transplantation
2) Dr. Gelovani, Professor and Chair, Experimental Diagnostic Imaging
3) Dr. Hwu, Professor, Chair, Melanoma Medical Oncology
4) Dr. Kleinerman, Professor, Division Head, Pediatrics
5) Dr. Liu, Professor, Chair, Immunology
6) Dr. Young, Associate Chief of Staff for Research Ralph H. Johnson VA Medical Center

The average scores are provided in Tables A and B below.

A transition plan has been developed per Section 14 "Supporting Documentation" of the original grant application. An optimization score has been developed from this feedback and is provided in Table C. In this first year of the grant award the technology has been developed and *in vitro* testing has been performed. The *in vivo* modeling will be undertaken in the second year and this will allow the optimization score to be determined.

[1] ljncooper@mdanderson.org
[2] leslopez@mdanderson.org

From the original grant application:
"...the committee will score the research since the last meeting for progress according to the Table A below using the following scale: 0 = no progress, 1 = adequate progress, 2 = progress beyond expectation, and 3 = exemplary progress. The committee will also assign an impact score according to Table B below using the following scale: 0 = no expected impact, 1 = impact expected to be adequate, 2 = impact likely to be beyond expectation, and 3 = impacted expected to be highly significant. These scores will be tabulated at each of the interim analyses and yearly meetings. To avoid bias, the PI, Dr. Cooper will not score the research, and the scoring will be anonymous. These scores as well as written comments from the committee members will be used to measure progress. Additional meetings may be requested by the PI, committee members and the DOD to discuss new data and plans, or if progress and impact has been less than expected as reflected by a downward trend in the scoring from Tables A and B."

Table A: Interim Progress Assessment	**Date = 05/07/2008**
Topic	**Score (0 to 3)**
Hypothesis/Task #1	3
Hypothesis/Task #2	3
Hypothesis/Task #3	3
Childhood cancer research	3
Blood-related cancer research	3
Military's needs	3
Veterans' needs	3
Total	21

Table B: Interim Impact Assessment	**Date = 05/07/2008**
Topic	**Score (0 to 3)**
Hypothesis/Task #1	3
Hypothesis/Task #2	3
Hypothesis/Task #3	3
Childhood cancer research	3
Blood-related cancer research	3
Military's needs	3
Veterans' needs	3
Total	21

Table C: Transition Plan for the Advanced Technology Development Funding							
		Mechanisms					
Task/ hypothesis	Product	*In vivo* persistence score[1]	*In vivo* efficacy score[2]	Synergy score[3]	Manufacturing score[4]	Regulatory score[5]	Optimization Score Total
1	Combining ICK and CD19-specific T cells	N/A	N/A	N/A	1	2	3
2	Combining CD19-specific $CD4^+$ T cells with $CD8^+$ T cells	N/A	N/A	N/A	2	3	5
3	$CD19RCD28^+$ T cells	N/A	N/A	N/A	3	1	4
Null	$CD19R^+$ T cells (1^{st}-generation)	1	1	0	4	4	10

[1] Which of the three hypotheses/tasks resulted in improved *in vivo* T-cell persistence? Score 4 points for each new therapy which resulted in longer *in vivo* persistence compared with infusion of 1^{st}-generation $CD19R^+$ T cells. Score 1 point if the 2^{nd}-generation technology is equivalent to the first, and no points if it is worse than the first.

[2] Which of the three hypotheses/tasks resulted in improved *in vivo* T-cell anti-tumor effect? Score 4 points for each new therapy which resulted in an improved *in vivo* anti-tumor effect compared with infusion of 1^{st}-generation $CD19R^+$ T cells. Score 1 point if the 2^{nd}-generation technology is equivalent to the first, and no points if it is worse than the first.

[3] Score 3 points if a hypothesis/task resulted in at least equivalent T-cell persistence and at least equivalent anti-tumor effect, compared with adoptive transfer of $CD19R^+$ T cells.

[4] The relative ease of manufacturing the new reagents will be reflected in the scoring. The scoring reflects the following hierarchy: (i) $CD19RCD28^+$ T cells (only one biologic product is needed), (ii) Combining CD19-specific $CD4^+$ T cells with CD19-specific $CD8^+$ T cells (both of these T-cell populations can be readily generated from a donor and genetic modification uses technology which is currently in clinical trials), (iii) Combining CD10-specific-IL2 ICK and CD19-specific T cells (requires generation of two products, one antibody-based reagent, and one cellular reagent). $CD19R^+$ T cells are already in clinical trials.

[5] Consideration will also be given to potential ease of obtaining regulatory approval. The *a priori* assumption is that some new technologies may be easier to obtain regulatory approval and this is reflected in the scoring in the table. $CD19R^+$ T cells are already in clinical trials.

INTEROFFICE MEMORANDUM

TO: US DEPARTMENT OF DEFENSE

FROM: LAURENCE COOPER[1]

CC: LESLIE LOPEZ[2]

DATE: 5/19/2008

SUBJECT: ANNUAL REPORT FOR DOD GRANT – CONCLUSION

Department: Pediatrics - Patient Care
Agency: US Department of Defense
Sponsor Number: W91ZSQ6289N610
Award Number: W81XWH-07-1-0250 01
Project Period: 04/15/2007- 05/15/2011
Title: Development of Augmented Leukemia/Lymphoma-Specific T-Cell Immunotherapy for Deployment with Haploidentical Hematopoietic Progenitor-Cell Transplant

In this first year of progress we have undertaken the *in vitro* studies to develop three approaches to improving the persistence of CD19-specific T cells. Two of these technologies will now be evaluated in animal models in the second year of the award.

[1] ljncooper@mdanderson.org
[2] leslopez@mdanderson.org

INTEROFFICE MEMORANDUM

TO: US DEPARTMENT OF DEFENSE

FROM: LAURENCE COOPER[1]

CC: LESLIE LOPEZ[2]

DATE: 5/19/2008

SUBJECT: ANNUAL REPORT FOR DOD GRANT - REFERENCES

Department: Pediatrics - Patient Care
Agency: US Department of Defense
Sponsor Number: W91ZSQ6289N610
Award Number: W81XWH-07-1-0250 01
Project Period: 04/15/2007- 05/15/2011
Title: Development of Augmented Leukemia/Lymphoma-Specific T-Cell Immunotherapy for Deployment with Haploidentical Hematopoietic Progenitor-Cell Transplant

Singh H, Serrano LM, Pfeiffer T, Olivares S, McNamara G, Smith DD, Al-Kadhimi Z, Forman SJ, Gillies SD, Jensen MC, Colcher D, Raubitschek A, Cooper LJN. Combining Adoptive Cellular and Immunocytokine Therapies to Improve Treatment of B-Lineage Malignancy. Cancer Res 67: (6), 2872-2880, 15 March 2007.

Singh H, Manuri PR, Olivares S, Dara N, Dawson MJ, Huls H, Hackett PB, Kohn DB, Shpall EJ, Champlin RE, Cooper LJN. Redirecting Specificity of T-Cell Populations For CD19 Using the Sleeping Beauty System. Cancer Res 68: (8), 2961-2971, 15 April 2008.

[1] ljncooper@mdanderson.org
[2] leslopez@mdanderson.org

Combining Adoptive Cellular and Immunocytokine Therapies to Improve Treatment of B-Lineage Malignancy

Harjeet Singh,[1,7] Lisa Marie Serrano,[1] Timothy Pfeiffer,[1] Simon Olivares,[1,7] George McNamara,[2] David D. Smith,[3] Zaid Al-Kadhimi,[1,4] Stephen J. Forman,[2,4] Stephen D. Gillies,[6] Michael C. Jensen,[2,4,5] David Colcher,[2] Andrew Raubitschek,[2] and Laurence J.N. Cooper[1,4,5,7]

Divisions of [1]Molecular Medicine, [2]Cancer Immunotherapeutics and Tumor Immunology, [3]Biomedical Informatics, [4]Hematology and Hematopoietic Cell Transplantation, and [5]Pediatric Hematology/Oncology, Beckman Research Institute and City of Hope National Medical Center; [6]EMD Lexigen Research Center, Billerica, Massachusetts; and [7]Division of Pediatrics, The University of Texas M. D. Anderson Cancer Center, Houston, Texas

Abstract

Currently, the lineage-specific cell-surface molecules CD19 and CD20 present on many B-cell malignancies are targets for both antibody- and cell-based therapies. Coupling these two treatment modalities is predicted to improve the antitumor effect, particularly for tumors resistant to single-agent biotherapies. This can be shown using an immunocytokine, composed of a CD20-specific monoclonal antibody fused to biologically active interleukin 2 (IL-2), combined with *ex vivo* expanded human umbilical cord blood–derived $CD8^+$ T cells, that have been genetically modified to be CD19 specific, for adoptive transfer after allogeneic hematopoietic stem-cell transplantation. We show that a benefit of targeted delivery of recombinant IL-2 by the immunocytokine to the $CD19^+CD20^+$ tumor microenvironment is improved *in vivo* persistence of the CD19-specific T cells, and this results in an augmented cell-mediated antitumor effect. Phase I trials are under way using anti-CD20-IL-2 immunocytokine and CD19-specific T cells as monotherapies, and our results warrant clinical trials using combination of these two immunotherapies. [Cancer Res 2007;67(6):2872–80]

Introduction

Malignant B cells express a pattern of cell surface molecules that define their lineage commitment (1–3), and these are the targets of monoclonal antibody (mAb)–based (4–6) and T-cell–based treatment approaches (7–11). However, these immunotherapies may fail to eradicate tumor as a result of an inability of tumor-specific mAb to fully activate the effector functions of the recipient (12–15) and curtailed T-cell persistence after adoptive immunotherapy (16–18). Therefore, strategies that augment mAb function and T-cell survival are predicted to improve the therapeutic effect.

An approach to improve the clinical potential of mAb is to fuse interleukin 2 (IL-2) to a tumor-specific recombinant mAb (e.g., CD20-specific mAb) to deliver this immunostimulatory cytokine to the tumor microenvironment, which leads to recruitment and activation of immune cells that express the cytokine receptor (19–21). *Ex vivo* propagated genetically modified T cells that have been rendered tumor specific are a population of effector cells whose survival is predicted to benefit from this locoregional deposition of IL-2.

To obtain large numbers of clinical-grade, tumor-specific T cells that target B-lineage lymphoma and leukemia, we and others have enforced expression of a CD19-specific chimeric immunoreceptor (designated CD19R), which combines antibody recognition with T-cell effector functions (7, 10, 22). In particular, CD19-specific T cells can be manufactured from umbilical cord blood to augment the graft-versus-tumor effect after allogeneic hematopoietic stem-cell transplantation (23). However, factors that may limit the successful therapeutic use of these *ex vivo* expanded $CD8^+$ T cells include a dependence on exogenous IL-2 to achieve and sustain their proliferative potential after adoptive transfer (24).

With the generation of an anti-CD20-IL-2 immunocytokine (DI-Leu16-IL-2; ref. 25), we now ask if targeted delivery of IL-2 to sites of CD20 binding on malignant B cells could improve the survival and antitumor effect of CD19-specific T cells. In the present study, we show that the anti-CD20-IL-2 immunocytokine binds specifically to $CD20^+$ tumors as well as $IL\text{-}2R^+$ (IL-2 receptor positive) T cells and that infusing a combination of anti-CD20-IL-2 immunocytokine with $CD19R^+$ T cells improves *in vivo* T-cell persistence, which leads to an augmented clearance of $CD20^+CD19^+$ tumor beyond that achieved by delivery of the immunocytokine or T cells alone.

Materials and Methods

Plasmid expression vectors. The plasmid vector CD19R/ffLucHyTK-pMG, described previously, coexpresses the *CD19R* chimeric immunoreceptor gene and the tripartite fusion gene *ffLucHyTK* (22). Truncated CD19, lacking the cytoplasmic domain (26), was expressed in ffLucHyTK-pMG to generate the plasmid tCD19/ffLucHyTK-pMG to coexpress the *CD19* and *ffLucHyTK* transgenes. The bifunctional *hRLucZeo* fusion gene that coexpresses the *Renilla koellikeri* (sea pansy) luciferase hRLuc and the zeomycin-resistance gene (*Zeo*) was cloned from the plasmid pMOD-LucSh (InvivoGen, San Diego, CA) into $pcDNA3.1^+$ (Invitrogen, Carlsbad, CA) to create the plasmid hRLuc:Zeocin-pcDNA3.1.

Propagation of cell lines and primary human T cells. Daudi, ARH-77, Raji, SUP-B15, and K562 cells were obtained from American Type Culture Collection (Manassas, VA). Granta-519 cells were obtained from DSMZ (Braunschweig, Germany). An EBV-transformed lymphoblastoid cell line was kindly provided by Drs. Phillip Greenberg and Stanley Riddell (Fred Hutchinson Cancer Research Center, Seattle, WA). These cells were maintained in tissue culture as described (23). $IL\text{-}2R\beta^+$ TF-1β cells were kindly provided by Dr. Paul M Sondel (University of Wisconsin, Madison, WI; ref. 27). Human T-cell lines were derived from umbilical cord blood mononuclear cells after informed consent and were cultured as previously described (22, 28).

Note: Supplementary data for this article are available at Cancer Research Online (http://cancerres.aacrjournals.org/).

Requests for reprints: Laurence J.N. Cooper, Pediatrics-Research, Unit 907, The University of Texas M. D. Anderson Cancer Center, 1515 Holcombe Boulevard, Houston, TX 77030. Phone: 713-563-3360; Fax: 713-563-0604; E-mail: ljncooper@mdanderson.org.

doi:10.1158/0008-5472.CAN-06-2283

Immunocytokines. The anti-CD20-IL-2 (DI-Leu16-IL-2) immunocytokine was derived from a deimmunized anti-CD20 murine mAb (Leu16). Anti-GD_2-IL-2 (14.18-IL-2), which recognized GD_2 disialoganglioside, served as a control immunocytokine with irrelevant specificity for B-lineage tumor line used in this study (EMD Lexigen Research Center, Billerica, MA; ref. 29).

Nonviral gene transfer of DNA plasmid vectors. OKT3-activated umbilical cord blood–derived T cells were genetically modified by electroporation with CD19R/ffLucHyTK-pMG (23). ARH-77 was electroporated with hRLuc:Zeocin-pcDNA3.1 using the Multiporator device (250V/40 μs, Eppendorf, Hamburg, Germany) and propagated in cytocidal concentration (0.2 mg/mL) of zeocin (InvivoGen).

Flow cytometry. FITC- or phycoerythrin-conjugated reagents were obtained from BD Biosciences (San Jose, CA): anti-TCRαβ, anti-CD3, anti-CD4, anti-CD8, anti-CD25, and anti-CD122. $F(ab')_2$ fragment of FITC-conjugated goat anti-human Fcγ (Jackson Immunoresearch, West Grove, PA) was used at 1/20 dilution to detect cell surface expression of *CD19R* transgene. Leu16 and anti-CD20-IL-2 immunocytokine (100 μg each) were conjugated to Alexa Fluor 647 (Molecular Probes, Eugene OR). Data acquisition was on a FACSCalibur (BD Biosciences) using CellQuest version 3.3 (BD Biosciences), and analysis was undertaken using FCS Express version 3.00.007 (Thornhill, Ontario, Canada).

Chromium release assay. The cytolytic activity of T cells was determined by 4-h chromium release assay (CRA; ref. 22). CD19-specific T cells were incubated with 5×10^3 chromium-labeled target cells in a V-bottomed 96-well plate (Costar, Cambridge, MA). The percentage of specific cytolysis was calculated from the release of ^{51}Cr, as described earlier, using a TopCount NXT (Perkin-Elmer Life and Analytical Sciences, Inc., Boston, MA). Data are reported as mean ± SD.

Immunofluorescence microscopy. $CD19R^+$ T cells (10^6) and $CD19^+$ $CD20^+$tumor cells (10^6) were centrifuged at 200 × *g* for 1 min and incubated at 37°C for 30 min. After gentle resuspension, the cells were sedimented, the supernatant was removed, and the pellet was fixed for 20 min with 3% parafomaldehyde in PBS on ice. After washing, the fixed T cell–tumor cell conjugates were incubated for 30 min at 4°C with anti-CD3-FITC or Alexa Fluor 647–conjugated anti-CD20-IL-2 immunocytokine. Nuclei were counterstained with Hoechst 33342 (Molecular Probes; 0.1 μg/mL). Cells were examined on a Zeiss LSM 510 META NLO Axiovert 200M inverted microscope. Hoechst 33342 was excited at 750 nm using Coherent Ti:Sapphire multiphoton laser, Alexa Fluor 647 at 633 nm using helium-neon laser, and FITC at 488 nm using argon ion laser. Images were acquired with a Zeiss plan-neofluar 20×/0.5 air lens or plan neofluar 40×/1.3 numerical aperture oil immersion lens, and fields of view were then examined using Zeiss LSM Image Browser version 3.5.0.223.

Persistence of adoptively transferred T cells. Before the initiation of the experiment, 6- to 10-week-old female NOD/*scid* (NOD/LtSz-*Prkdcscid*/J) mice (The Jackson Laboratory, Bar Harbor, ME) were γ-irradiated to 2.5 Gy using an external ^{137}Cs source (JL Shepherd Mark I Irradiator, San Fernando, CA) and maintained under pathogen-free conditions at City of Hope National Medical Center (COH) Animal Resources Center. On day −7, the mice were injected in the peritoneum with 2×10^6 $hRLuc^+$ $CD19^+CD20^+$ARH-77 cells. Tumor engraftment was evaluated by biophotonic imaging (see "Biophotonic imaging") and mice with progressively growing tumors were segregated into four treatment groups to receive 10^7 CD19-specific T cells (day 0) either alone or in combination with 75,000 units/injection (equivalent to ~25 μg immunocytokine; ref. 25) of IL-2 (Chiron, Emeryville, CA), 5 μg/injection of anti-CD20-IL-2 immunocytokine (DI-Leu16-IL-2), or 5 μg/injection of anti-GD_2-IL-2 immunocytokine, given by additional separate i.p. injections. Animal experiments were approved by COH institutional committees.

***In vivo* efficacy of combination immunotherapies.** Six- to 10-week-old γ-irradiated NOD/*scid* mice were injected with 2×10^6 $hRLuc^+$ $CD19^+CD20^+$ARH-77 cells in the peritoneum. Sustained tumor engraftment was documented within 7 days of injection by biophotonic imaging. Mice in the four treatment groups received combinations of CD19-specific T cells (10^7 cells in the peritoneum on day 0), anti-CD20-IL-2 immunocytokine, or anti-GD_2-IL-2 immunocytokine (5 μg/injection in the peritoneum).

Biophotonic imaging. Anesthetized mice were imaged using a Xenogen IVIS 100 series system as previously described (30). Briefly, each animal was serially imaged in an anterior-posterior orientation at the same relative time point after 100 μL (0.068 mg/mouse) of freshly diluted Enduren Live Cell Substrate (Promega, Madison, WI), or 150 μL (4.29 mg/mouse) of freshly thawed D-luciferin potassium salt (Xenogen, Alameda, CA) solution injection. Photons were quantified using the software program Living Image (Xenogen). Statistical analysis of the photon flux at the end of the experiment was accomplished by comparing area under the curve using two-sided Wilcoxon rank sum test. Biological T-cell half-life was calculated as $A = I \times (1/2)^{(t/h)}$, where A is flux at time t, I is day 0 flux, and h is rate of decay.

Results

Redirecting T cells specificity for CD19. The genetic modification of umbilical cord blood–derived T cells to render them specific for CD19 was accomplished by nonviral electrotransfer of a DNA expression plasmid designated CD19R/ffLucHyTK-pMG, which codes for the *CD19R* transgene (22) and a recombinant multifunction fusion gene that combines firefly luciferase (*ffLuc*), hygromycin phosphotransferase, and herpes virus thymidine kinase (*HyTK*; ref. 31), permitting *in vitro* selection of $CD19R^+$ T cells with cytocidal concentration of hygromycin B and *in vivo* imaging after infusion of D-luciferin. Genetically modified *ex vivo* expanded T cells were $CD8^+$, expressed components of the high-affinity IL-2R and *CD19R* transgene, as detected by using a Fc-specific antibody (Fig. 1*A*). $CD19R^+$ T cells could specifically lyse leukemia and lymphoma targets expressing CD19 with ~50% to 70% of $CD19^+$ tumor cells killed at an effector to target ratio of 50:1 in a 4 h CRA (Fig. 1*B*). The variability of lysis of the various B-cell lines could be attributed to the expression of various cell surface markers, particularly the adhesion molecules (22). Specific lysis of $CD19^+$ K562 compared with $CD19^-$ K562 cells showed that the killing of $CD19^+$ tumor targets occurred through the chimeric immunoreceptor.

Binding of anti-CD20-IL-2 immunocytokine. The ability of the anti-CD20-IL-2 immunocytokine to bind to both B-lineage tumors and T cells was examined using flow cytometry and confocal microscopy. This immunocytokine bound to $CD20^+$ ARH-77 but not to $CD20^-$ SUP-B15 (data not shown) and K562 cells, consistent with recognition of parental Leu16 mAb for CD20 (Fig. 2*A*; ref. 32). The anti-CD20-IL-2 immunocytokine, but not parental Leu16 mAb, bound to $CD25^+$ genetically modified T cells and TF-1β, a tumor cell line genetically modified to express CD122 (IL-2Rβ; ref. 27), which is consistent with binding of chimeric IL-2 via the IL-2R (Fig. 2*A* and data not shown). The greater median fluorescent intensity (MFI) on T cells, compared with TF-1β, is consistent with binding of the immunocytokine to the high-affinity IL-2R. Immunofluorescence confocal microscopy was done to evaluate the localization of immunocytokine on conjugates of CD19-specific T cells and $CD20^+$ tumors. The confocal micrographs showed cell surface labeling of conjugates of tumor and T cells with Alexa Fluor 647–conjugated anti-CD20-IL-2 immunocytokine (*red*) and T cells labeled with FITC-conjugated anti-CD3 (*green*). Areas of overlapping binding between deposition of immunocytokine and anti-CD3 is depicted by a yellow color (Fig. 2*B*). We hypothesize that T cells show colocalization of CD3 and immunocytokine on their surface initially; however, as they form a synapse with the tumor cell, there seems to be a rearrangement of IL-2R on the T cells toward the synapse leading to the presence of yellow signal extending well outside the synapse and leaving a green pocket opposite the synapse. The Alexa Fluor 647–conjugated parental

anti-CD20 Leu16 mAb, lacking the chimeric IL-2 domain, binds $CD20^+$ tumors, but not the genetically modified T cells (data not shown). In aggregate, these data show that anti-CD20-IL-2 immunocytokine can bind to CD20 molecules on B-lineage tumors and IL-2R on T cells and that this immunocytokine can be deposited at the interface between tumor and T cells.

***In vivo* T-cell persistence given in combination with immunocytokine.** Having determined that the anti-CD20-IL-2 immunocytokine could bind to tumor and T cells, we evaluated whether infusions of anti-CD20-IL-2 immunocytokine could improve the *in vivo* persistence of adoptively transferred genetically modified $CD8^+$ T cells. To achieve sustained locoregional

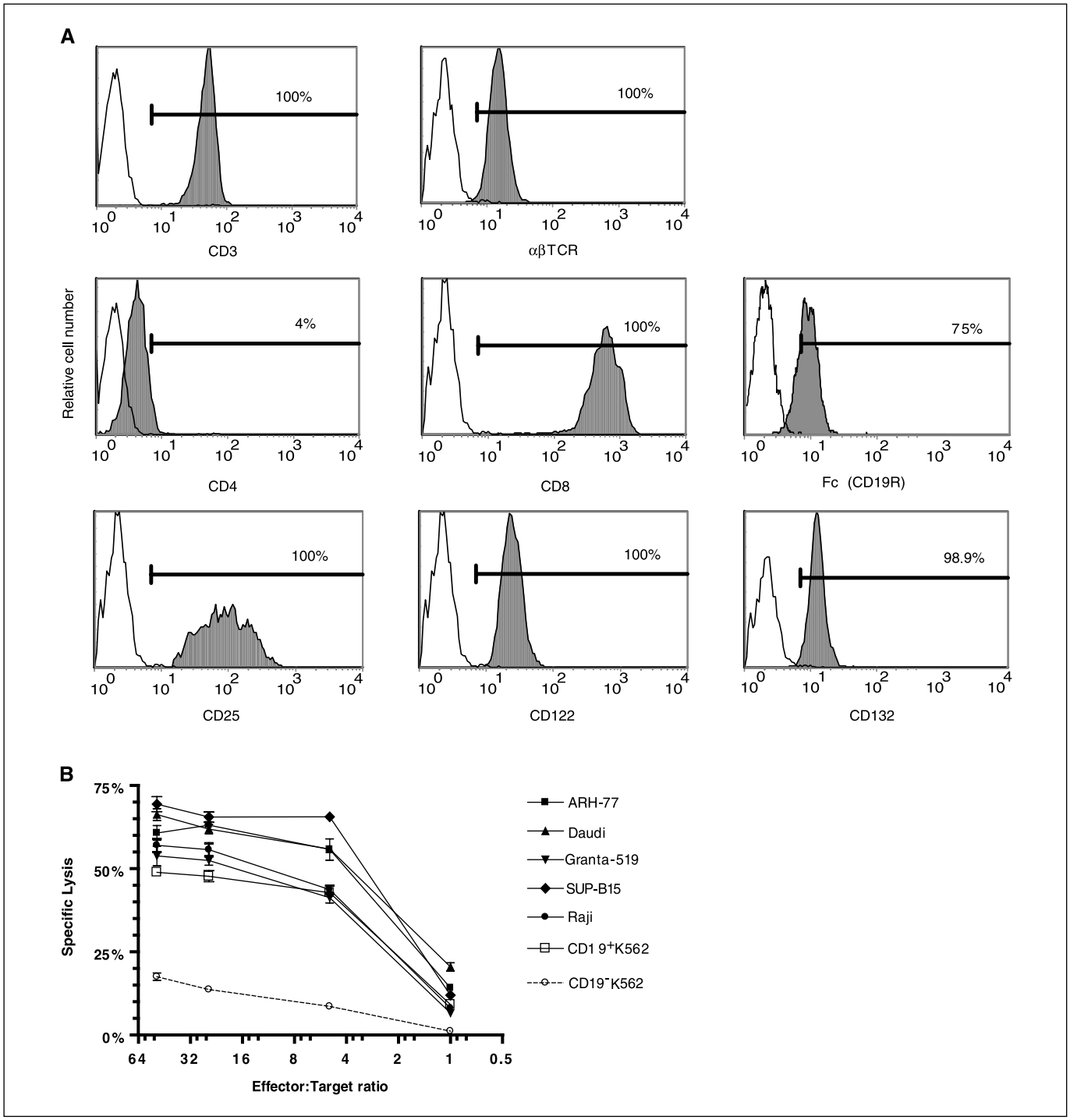

Figure 1. Phenotype and function of genetically modified T cells. *A,* multivariable flow cytometry showing that the genetically modified T cells are predominantly $CD3^+TCR^+CD8^+CD25^+CD122^+CD132^+$. Isotype-matched fluorescent mouse mAb or nonspecific goat control antibody was used to establish the negative gates. The percentage of gated$^+$ cells is shown. *B,* lysis of tumor targets by 4-h CRA. $CD19^+$ B-cell tumor lines are Daudi, ARH-77, SUP-B15, Granta-519, Raji, and genetically modified K562 ($CD19^+$ K562; ref. 30). Background lysis of $CD19^-$ (parental) K562 cells is shown as a control for specificity and endogenous NK-T activity. Spontaneous release of each target was ≤9%. *Points,* mean for triplicate wells at effector to target cell ratios between 50:1 and 1:1; *bars,* ± 1 SD.

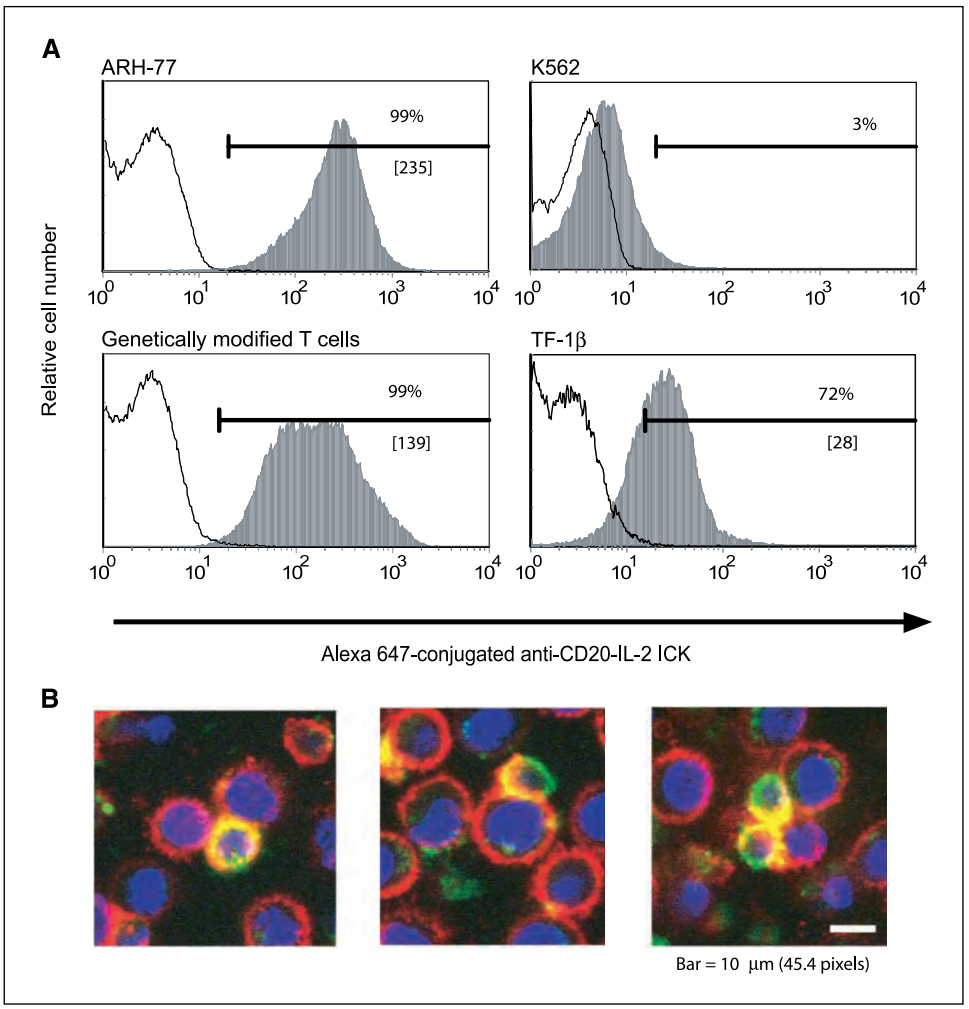

Figure 2. Binding of anti-CD20-IL-2 immunocytokine to B cells and T cells. *A,* flow cytometry analysis of Alexa Fluor 647–conjugated anti-CD20-IL-2 immunocytokine (ICK) binding through CD20 to $CD20^+CD25^-$ ARH-77 and $CD20^-CD25^-$ K562 cell lines; and IL-2 receptors to genetically modified $CD20^-CD25^+$ T cells and $CD20^-CD25^-CD122^+$ TF-1β (*filled histograms*). *Unfilled histograms,* fluorescence of unstained cells. The percentage of gated$^+$ cells and MFI (*in brackets*) are indicated. Alexa Fluor 647 emission (668 nm) was revealed in the APC/Cy5 channel (FL-4). *B,* confocal micrographs of tumor and T-cell conjugates stained with Alexa Fluor 647–conjugated anti-CD20-IL-2 immunocytokine (*red*) and FITC-conjugated anti-CD3 (*green*); cell nuclei were counterstained with Hoechst (*blue*). *Yellow,* areas that show overlapping binding of immunocytokine and anti-CD3 mAb.

depositions of the anti-CD20-IL-2 immunocytokine, we chose the tumor line ARH-77 as a target for immunotherapy because this is relatively resistant to killing by anti-CD20–specific mAb (33), and these results were confirmed *in vivo* in NOD/*scid* mice using rituximab (data not shown). Initially, a dose of immunocytokine was established that could both improve the *in vivo* survival of $CD8^+CD19R^+ffLuc^+$ T cells, compared with adoptive immunotherapy in the absence of immunocytokine, and not statistically alter tumor growth as monotherapy (Fig. 4). We showed that an immunocytokine dose of both 5 and 25 μg could improve the persistence of infused T cells, resulting in a T-cell ffLuc-derived signal detectable above background luminescence measurements ($\leq 10^6$ p/s/cm^2/sr) 14 days after adoptive immunotherapy (Fig. 3*A*). Biological half-life of the infused T cells was determined by calculating the rate of T-cell decay (ffLuc activity) at the end of the experiment and expressed as the number of days required by the cells to achieve half the initial (day 0) flux. Indeed, the biological half-life of the infused T cells was twice as long in mice that received immunocytokine (1.09 days) compared with T cells given alone (0.43 days). As a further indication that infusion of the immunocytokine may enhance the survival of adoptively transferred T cells, we observed an ~300% (3-fold) increase in the ffLuc-derived signal (day 12) compared with day 11 when the immunocytokine was injected in both the groups. As the relative *in vivo* T-cell persistence was similar for both of the immunocytokine doses (P = 0.86), we used 5 μg per immunocytokine injection for subsequent experiments, a dose equivalent to ~15,000 units of human recombinant IL-2 (25).

To determine if the improved T-cell persistence was due to the binding of the immunocytokine in the ARH-77 tumor microenvironment, we used a control immunocytokine (anti-GD_2-IL-2 immunocytokine) that does not bind to GD_2^- ARH-77 (data not shown). Furthermore, we compared the ability of the anti-CD20-IL-2 immunocytokine to potentiate T-cell survival compared with administration of exogenous recombinant human IL-2. Longitudinal measurement of ffLuc-derived flux revealed that the infused T cells persisted longer in mice that received anti-CD20-IL-2 immunocytokine, compared with the untreated (P = 0.01), IL-2–treated (P = 0.02), and control immunocytokine-treated (P = 0.05) groups (Fig. 3*B* and *C*); the biological half-lives of T cells in the groups are 1.7, 0.5, 1.0, and 0.7 days, respectively. There was a difference (P < 0.05) in the *in vivo* persistence of T cells accompanied by IL-2, compared with T cells given without this cytokine, which is consistent with the dependence of these T cells to receive T-cell help in the form of exogenous IL-2 to survive *in vivo*. No apparent difference was observed in the persistence (P = 0.5) or biological half-life (P = 0.2) of adoptively transferred T cells between the mice receiving exogenous IL-2 or control immunocytokine. These data support the hypothesis that the locoregional deposition of the anti-CD20-IL-2 immunocytokine at

the $CD19^+CD20^+$ tumor site significantly augments *in vivo* persistence of $CD8^+$ CD19-specific T cells.

***In vivo* efficacy of immunocytokine in combination with CD19-specific T cell to treat established B-lineage tumor.** We investigated *in vivo* whether the immunocytokine-mediated improved persistence of genetically modified CD19-specific T cells could lead to augmented clearance of established $CD19^+CD20^+$ tumor. A dose of T cells (10^7 cells) was selected because this dose by itself does not control long-term tumor growth (Fig. 4; data not shown). CD19-specific $CD8^+$ T cells were adoptively transferred into groups of mice bearing established $CD19^+CD20^+hRLuc^+$ ARH-77 tumor along with anti-CD20-IL-2 immunocytokine or control anti-GD_2-IL-2 immunocytokine. Tumor growth was serially monitored by *in vivo* bioluminescence imaging of ARH-77 tumor-derived hRLuc enzyme activity. Mice that received both CD19-specific T cells and anti-CD20-IL-2 immunocytokine experienced a reduction in tumor growth, with 75% of mice obtaining complete remission, as measured by bioluminescence imaging, at the end of

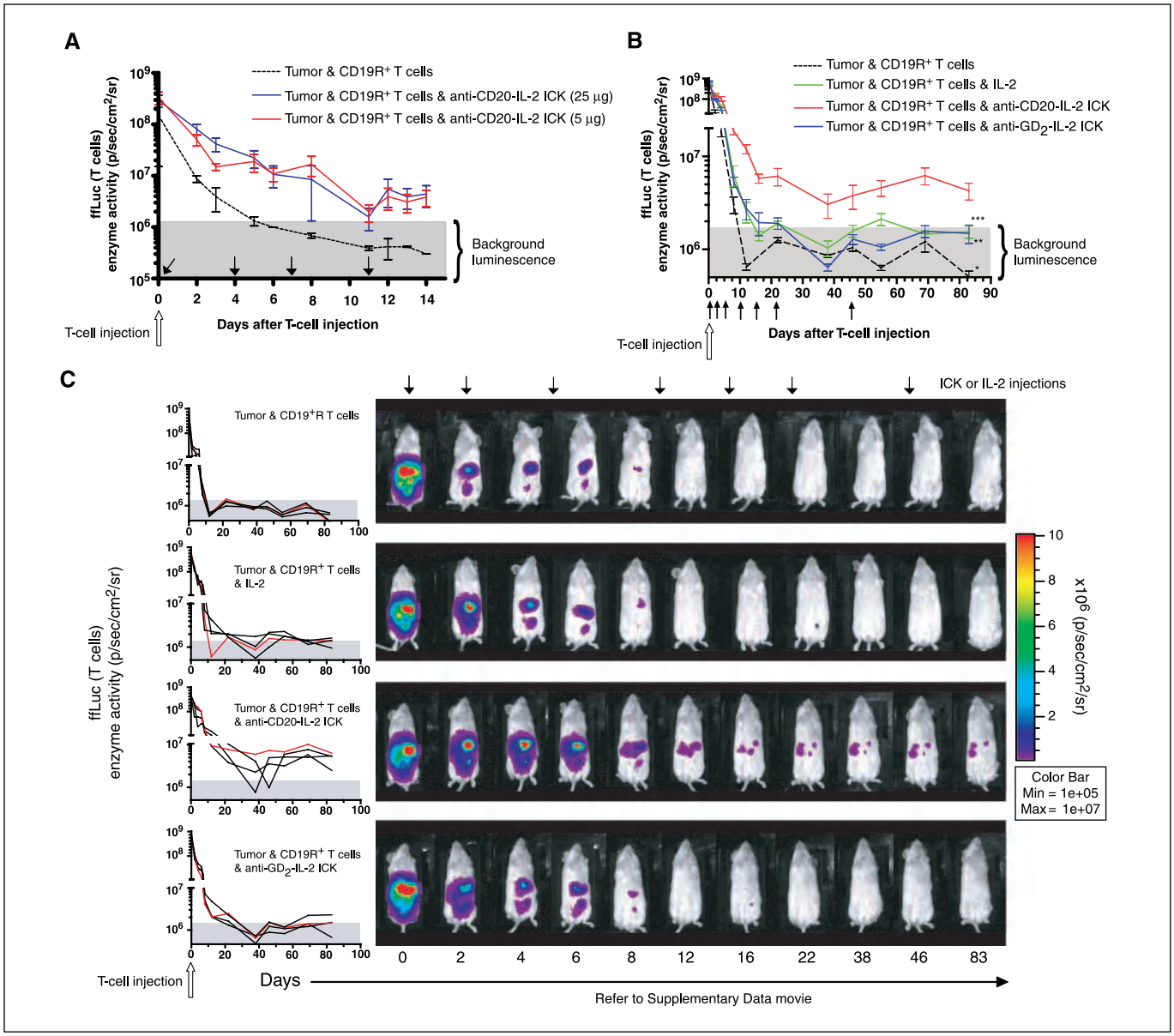

Figure 3. Effect of immunocytokine on persistence of adoptively transferred T cells. NOD/*scid* mice (four mice per group) bearing ARH-77 tumors were treated with 10^7 $CD19R^+ffLuc^+$ umbilical cord blood T-cell clone (day 0, *open arrow*) along with (*A*) anti-CD20-IL-2 immunocytokine (5 and 25 μg; *solid arrows*; on days 0, 4, 7, and 11) or no immunocytokine, or (*B*) anti-CD20-IL-2 immunocytokine/GD_2-IL-2 immunocytokine (5 μg/injection) or rhIL-2 (75,000 units/injection) on days 0, 2, 5, 10, 15, 21, and 45 (*closed arrows*). The persistence of T cells was measured as ffLuc-derived flux from mice and graphed over time (mean flux ± SD is shown in *A* and *B*, and flux for individual mice is shown in *C*). One mouse (*red line*) was selected from each group for the display of sequential bioluminescence images of T cells *in vivo*. Comparison (day 83) between groups receiving combination of T cells and anti-CD20-IL-2 immunocytokine and no treatment (*, $P = 0.01$); T cells and control immunocytokine (anti-GD_2-IL-2 immunocytokine; **, $P = 0.05$); or T cells and IL-2 (***, $P = 0.02$). Background luminescence (*gray area*) was defined from mice that were imaged after receiving D-luciferin along with treatment mice, but which did not receive $ffLuc^+$ T cells. *In vitro* ffLuc activity of the genetically modified T cells was 0.35 ± 0.02 cpm/cell (mean ± SD) compared with 0 ± 0 cpm/cell (mean ± SD) for parental unmodified cells. Supplementary Data contain a movie of the relative *in vivo* T-cell persistence in the four treatment groups.

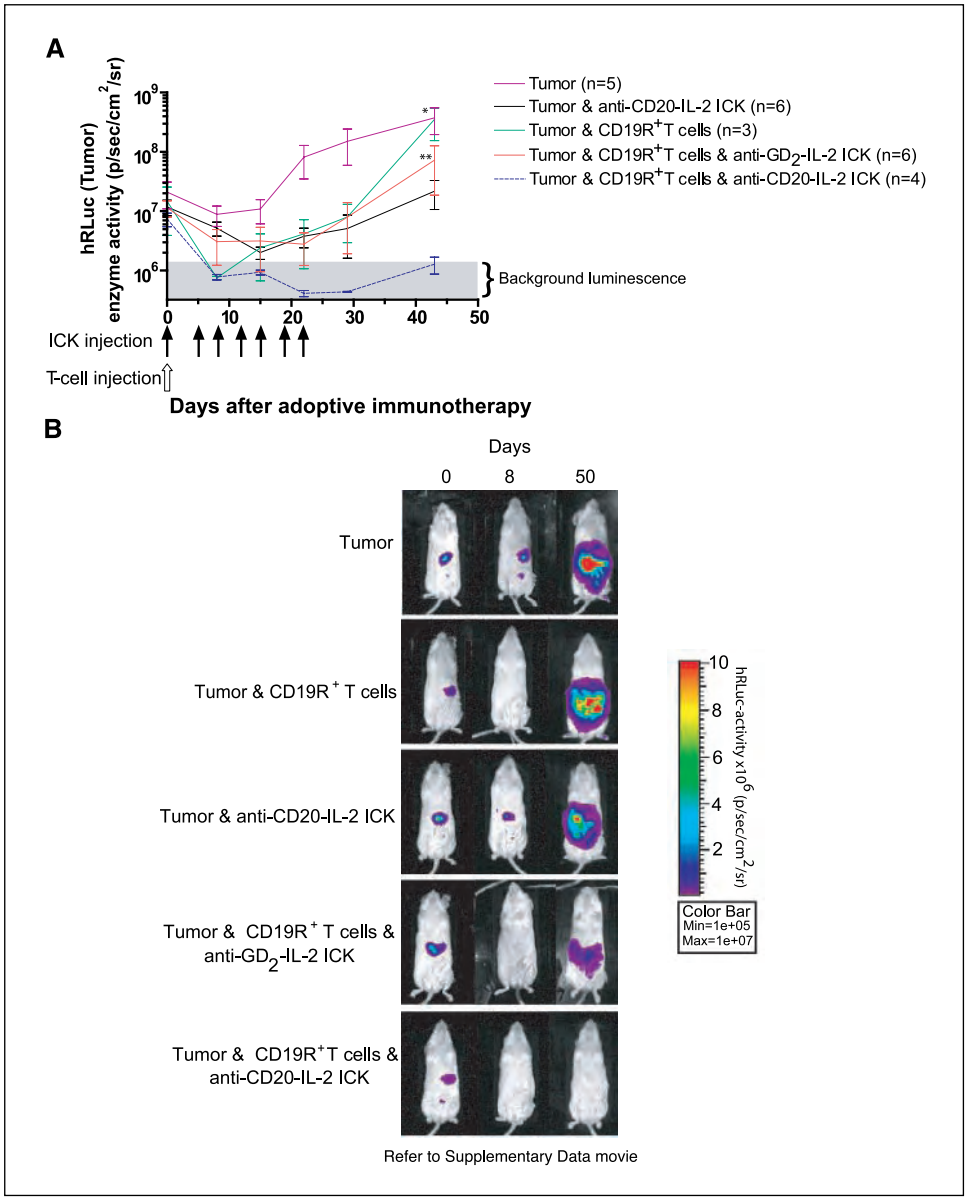

Figure 4. Combined antitumor efficacy of immunocytokine and CD19-specific T cells. *A,* the tumor burden was monitored longitudinally by quantification of ARH-77 tumor-derived hRLuc activity in five groups of NOD/*scid* mice receiving combinations of T cells (10^7 on day 0, *open arrow*); anti-CD20-IL-2 immunocytokine (5 μg/injection); anti-GD_2-IL-2 immunocytokine (5 μg/injection) given on days 0, 5, 8, 12, 15, 19, and 22 (*closed arrows*); and graphed over time as mean flux ± SD. *B,* serial pseudocolor images representing light intensity from hRLuc ARH-77 cells in selected mice before and after immunotherapy. Comparison (day 50) between groups receiving combination of T cells and anti-CD20-IL-2 immunocytokine and no treatment (*, $P = 0.01$), and T cells and control immunocytokine (anti-GD_2-IL-2 immunocytokine; **, $P = 0.03$). Genetically modified ARH-77 (transfected with hRLuc:Zeocin-pcDNA3.1) hRLuc activity *in vitro* was 0.32 ± 0.04 cpm/cell (mean ± SD) compared with 0.004 ± 0.0008 cpm/cell (mean ± SD) for parental unmodified cells. Supplementary Data contain a movie of the relative *in vivo* antitumor effects of immunotherapy in the five mouse groups.

the experiment (50 days after adoptive immunotherapy; Fig. 4). We found that the combination therapy of $CD19R^+$ T cells and anti-CD20-IL-2 immunocytokine was effective in reducing tumor growth compared with no immunotherapy ($P = 0.01$) and T cells given with an equivalent dosing of the control immunocytokine ($P = 0.03$). Although the tumor burden seems to be increasing in the treated group, no visible tumor as seen by hRLuc signal was observed at the end of the experiment, as the flux remained below background level, consistent with a complete antitumor response. Mouse groups receiving T cells alone or T cells with control immunocytokine showed a similar pattern of tumor growth, with an initial reduction around day 8 followed by relapse. All mice in the control group, which received no immunotherapy, experienced sustained tumor growth. We saw similar tumor growth kinetics in mice that did or did not receive anti-CD20-IL-2 immunocytokine in the absence of T cells ($P > 0.05$ through day 50), and this is presumably a reflection of the dose regimen chosen for the immunocytokine in this experiment. Increased doses of T cells or anti-CD20-IL-2 immunocytokine delivered as monotherapies results in a sustained antitumor effect; however, using these doses would preclude our ability to measure the ability of the immunocytokine to potentiate T-cell persistence and improve tumor killing.

The ability to measure both ffLuc and hRLuc enzyme activities in the same mice allowed us to determine whether the persistence of adoptively transferred T cells directly correlated with tumor size for individual mice. This was accomplished by plotting ffLuc-derived T-cell flux versus hRLuc-derived tumor-cell flux from Fig. 3. Both group of mice, which received CD19-specific T cells along with anti-CD20-IL-2 immunocytokine/anti-GD_2-IL-2 immunocytokine, showed a drop in tumor burden at day 8, which is due to the T cells infused. However, the highest numbers of T cells (ffLuc activity; mean flux 4.7×10^6 versus 1.5×10^6 p/s/cm^2/sr) and lowest tumor burden (hRLuc activity; mean flux 1.4×10^7 versus 4×10^7 p/s/cm^2/sr) by day 83 (Fig. 5) was observed in the group receiving anti-CD20-IL-2 immunocytokine when compared with

the control immunocytokine-treated group. This analysis shows that half of the mice achieved an antitumor response (absence of detectable hRLuc activity) after combination immunotherapy with CD19R$^+$ T cells and anti-CD20-IL-2 immunocytokine. We note that there was continued T-cell persistence (ffLuc activity) in the anti-CD20-IL-2 immunocytokine–treated group compared with the control immunocytokine–treated group ($P < 0.05$) at day 83. Although tumor burden (hRLuc activity) was reduced in the CD20 immunocytokine– compared with the control immunocytokine–treated group at day 83, no statistical significance was observed. Thus, we note a trend toward continued T-cell persistence and desired antitumor effect in the anti-CD20-IL-2 immunocytokine–treated group.

We believe that this is the first time that bioluminescence imaging has been used to connect the persistence of genetically modified T cells to an antitumor effect. These data further reveal that the mice that received the tumor-specific immunocytokine control their tumor burden to a greater extent than the mice that received the control immunocytokine (which does not bind the tumor). As a treatment for minimal residual disease in patients undergoing hematopoietic stem-cell transplantation, this combination therapy shows the ability to keep the disease relapse in check for almost 3 months in this mouse model.

In aggregate, these data show that the combination of anti-CD20-IL-2 immunocytokine and CD19R$^+$ T cells results in augmented control of tumor growth, as predicted from the *in vivo* T-cell persistence data.

Discussion

We show that anti-CD20-IL-2 immunocytokine specifically binds to CD20$^+$ tumor, that infusions of the anti-CD20-IL-2 immunocytokine can augment persistence of adoptively transferred CD19-specific T cells *in vivo*, and that this leads to improved control of an established CD19$^+$CD20$^+$ tumor. We believe that these observations are due to the deposition of IL-2 at sites of CD20 binding, which provides a positive survival stimulus to infused CD19R$^+$IL-2R$^+$ effector T cells residing in the tumor microenvironment.

The development of an anti-CD20-IL-2 immunocytokine has implications for future immunotherapy of B-lineage malignancies. Although rituximab has been extensively used to treat CD20$^+$ malignancies (34–36), some patients become unresponsive to this mAb therapy, leading to disease progression (37). The development of an anti-CD20-IL-2 immunocytokine with its ability to activate immune effector cells may rescue these patients, and a clinical trial at COH is under way to determine the safety and feasibility of infusing this immunocytokine. Modifications other than the addition of cytokines (38, 39), such as radionucleotides (40) and cytotoxic agents (41, 42), may also improve the therapeutic potential of unconjugated clinical-grade mAbs. Indeed, combining mAb therapy with therapeutic modalities that exhibit nonoverlapping toxicity profiles is an attractive strategy to improve the antitumor effect without compromising patient safety.

One novel combination therapy for treating B-lineage tumors, described in this report, is to combine immunocytokine with T-cell therapy. The two immunotherapies used, anti-CD20-IL-2 immunocytokine and CD19-specific T cells, have the potential to improve the eradication of tumor because (*a*) the targeting of different cell surface molecules reduces the possibility emergence of antigen-escape variants, (*b*) the mAb conjugated to IL-2 can recruit and activate effector cells (such as CD19-specific T cells) expressing the cytokine receptor in the tumor microenvironment, and (*c*) T cells

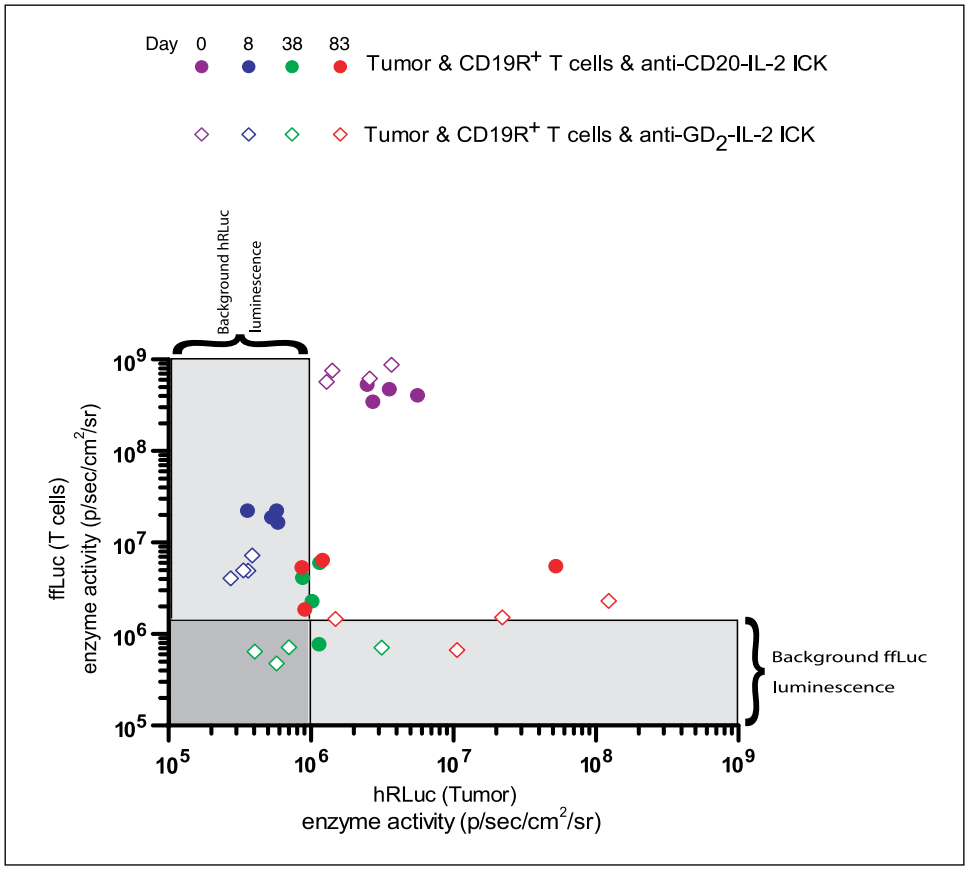

Figure 5. Measurement of both T-cell persistence and antitumor effect of immunotherapies in individual mice. Mice were treated as in Fig. 3*B*, and T-cell persistence (ffLuc signal, *Y axis*) along with tumor burden (hRLuc signal, *X axis*) was measured in the same mouse at the days mentioned. Improved T-cell persistence (ffLuc signal) and reduced tumor burden (antitumor effect, hRLuc signal) in mice that received a combination of CD19-specific T cells and anti-CD20-IL-2 immunocytokine is observed at day 83. *Shaded gray areas,* background fluorescence.

can kill independent of host factors, which may limit the effectiveness of mAb-mediated complement dependent cytotoxicity and antibody-dependent cell cytotoxicity (12–15). These immunotherapies will target both malignant and normal B cells. However, as loss of normal B-cell function has not been an impediment to rituximab therapy and as clinical conditions associated with hypogammaglobulinemia could be corrected with infusions of exogenous immunoglobulin, a loss of B-cell function may be an acceptable side effect in patients with advanced B-cell leukemias and lymphomas receiving CD19- and/or CD20-directed therapies.

Another potential advantage of immunocytokine therapy is that the locoregional delivery of T-cell help in the form of IL-2 may avoid the systemic toxicities observed with i.v. infusion of the IL-2 cytokine (43–45), and this may be particularly beneficial in the context of allogeneic hematopoietic stem-cell transplantation. We have recently described that umbilical cord blood–derived $CD8^+$ T cells can be rendered specific for CD19 to augment the graft-versus-tumor effect after hematopoietic stem-cell transplantation. Moreover, because the immunocytokine improves the *in vivo* immunobiology of umbilical cord blood–derived CD19-specific T cells, this study provides the groundwork for combining these two immunotherapies after umbilical cord blood transplantation.

Alternative immunocytokines and T cells with shared specificities for tumor types other than B-lineage malignancies could also be considered for combination immunotherapy. For example, immunocytokines might be combined with T cells that have been rendered specific by the introduction of chimeric immunoreceptors for breast (46, 47), ovarian (48), colon (49), and brain (50) malignancies. Furthermore, immunocytokines bearing other cytokines might be infused with T cells to deliver IL-7, IL-15, or IL-21 to further augment T-cell function in the tumor microenvironment.

In summary, the clinical testing of anti-CD20-IL-2 immunocytokine and $CD19R^+$ T cells as monotherapy will provide Phase I safety and feasibility data. It is anticipated that the data in this report will be used to justify next-generation clinical trials to evaluate combinations of the immunocytokine and T cells.

Acknowledgments

Received 6/21/2006; revised 12/4/2006; accepted 1/3/2007.

Grant support: CA30206, CA003572, and CA107399; Alliance for Cancer Gene Therapy; Amy Phillips Charitable Foundation; The Leukemia and Lymphoma Society; Lymphoma Research Foundation; National Foundation for Cancer Research; Pediatric Cancer Research Foundation; National Marrow Donor Program; and Marcus Foundation.

The costs of publication of this article were defrayed in part by the payment of page charges. This article must therefore be hereby marked *advertisement* in accordance with 18 U.S.C. Section 1734 solely to indicate this fact.

We thank Adrian Castro and Vanessa Reeves for assistance with animal experiments, COH Animal Resource Center (under the direction of Dr. Richard Ermel), and the Light Microscopy and Flow Cytometry Cores.

References

1. Stamenkovic I, Seed B. CD19, the earliest differentiation antigen of the B cell lineage, bears three extracellular immunoglobulin-like domains and an Epstein-Barr virus-related cytoplasmic tail. J Exp Med 1988;168:1205–10.
2. Tedder TF, Streuli M, Schlossman SF, Saito H. Isolation and structure of a cDNA encoding the B1 (CD20) cell-surface antigen of human B lymphocytes. Proc Natl Acad Sci U S A 1988;85:208–12.
3. Wortis HH. Surface markers, heavy chain sequences and B cell lineages. Int Rev Immunol 1992;8:235–46.
4. Cragg MS, Walshe CA, Ivanov AO, Glennie MJ. The biology of CD20 and its potential as a target for mAb therapy. Curr Dir Autoimmun 2005;8:140–74.
5. Scheuermann RH, Racila E. CD19 antigen in leukemia and lymphoma diagnosis and immunotherapy. Leuk Lymphoma 1995;18:385–97.
6. Weiner GJ, Link BK. Monoclonal antibody therapy of B cell lymphoma. Expert Opin Biol Ther 2004;4:375–85.
7. Brentjens RJ, Latouche JB, Santos E, et al. Eradication of systemic B-cell tumors by genetically targeted human T lymphocytes co-stimulated by CD80 and interleukin-15. Nat Med 2003;9:279–86.
8. Cheadle EJ, Gilham DE, Thistlethwaite FC, Radford JA, Hawkins RE. Killing of non-Hodgkin lymphoma cells by autologous CD19 engineered T cells. Br J Haematol 2005; 129:322–32.
9. Imai C, Mihara K, Andreansky M, et al. Chimeric receptors with 4-1BB signaling capacity provoke potent cytotoxicity against acute lymphoblastic leukemia. Leukemia 2004;18:676–84.
10. Roessig C, Scherer SP, Baer A, et al. Targeting CD19 with genetically modified EBV-specific human T lymphocytes. Ann Hematol 2002;81 Suppl 2:42–3.
11. Rossig C, Pscherer S, Landmeier S, Altvater B, Jurgens H, Vormoor J. Adoptive cellular immunotherapy with CD19-specific T cells. Klin Padiatr 2005;217:351–6.
12. Multani PS, Grossbard ML. Monoclonal antibody-based therapies for hematologic malignancies. J Clin Oncol 1998;16:3691–710.
13. Schmitt CA, Schwaeble W, Wittig BM, Meyer zum Buschenfelde KH, Dippold WG. Expression and regulation by interferon-γ of the membrane-bound complement regulators CD46 (MCP), CD55 (DAF) and CD59 in gastrointestinal tumours. Eur J Cancer 1999;35:117–24.
14. Treon SP, Shima Y, Preffer FI, et al. Treatment of plasma cell dyscrasias by antibody-mediated immunotherapy. Semin Oncol 1999;26:97–106.
15. Zhao S, Asgary Z, Wang Y, Goodwin R, Andreeff M, Younes A. Functional expression of TRAIL by lymphoid and myeloid tumour cells. Br J Haematol 1999; 106:827–32.
16. Dudley ME, Wunderlich JR, Robbins PF, et al. Cancer regression and autoimmunity in patients after clonal repopulation with antitumor lymphocytes. Science 2002; 298:850–4.
17. Klebanoff CA, Finkelstein SE, Surman DR, et al. IL-15 enhances the *in vivo* antitumor activity of tumor-reactive $CD8^+$ T cells. Proc Natl Acad Sci U S A 2004;101: 1969–74.
18. Minamoto S, Treisman J, Hankins WD, Sugamura K, Rosenberg SA. Acquired erythropoietin responsiveness of interleukin-2-dependent T lymphocytes retrovirally transduced with genes encoding chimeric erythropoietin/interleukin-2 receptors. Blood 1995;86:2281–7.
19. King DM, Albertini MR, Schalch H, et al. Phase I clinical trial of the immunocytokine EMD 273063 in melanoma patients. J Clin Oncol 2004;22:4463–73.
20. Lode HN, Xiang R, Becker JC, Gillies SD, Reisfeld RA. Immunocytokines: a promising approach to cancer immunotherapy. Pharmacol Ther 1998;80:277–92.
21. Sondel PM, Hank JA, Gan J, Neal Z, Albertini MR. Preclinical and clinical development of immunocytokines. Curr Opin Investig Drugs 2003;4:696–700.
22. Cooper LJ, Topp MS, Serrano LM, et al. T-cell clones can be rendered specific for CD19: toward the selective augmentation of the graft-versus-B-lineage leukemia effect. Blood 2003;101:1637–44.
23. Serrano LM, Pfeiffer T, Olivares S, et al. Differentiation of naive cord-blood T cells into CD19-specific cytolytic effectors for posttransplantation adoptive immunotherapy. Blood 2006;107:2643–52.
24. Dudley ME, Rosenberg SA. Adoptive-cell-transfer therapy for the treatment of patients with cancer. Nat Rev Cancer 2003;3:666–75.
25. Gillies SD, Lan Y, Williams S, et al. An anti-CD20-IL-2 immunocytokine is highly efficacious in a SCID mouse model of established human B lymphoma. Blood 2005; 105:3972–8.
26. Mahmoud MS, Fujii R, Ishikawa H, Kawano MM. Enforced CD19 expression leads to growth inhibition and reduced tumorigenicity. Blood 1999;94:3551–8.
27. Farner NL, Voss SD, Leary TP, et al. Distinction between γc detection and function in YT lymphoid cells and in the granulocyte-macrophage colony-stimulating factor-responsive human myeloid cell line, Tf-1. Blood 1995;86:4568–78.
28. Riddell SR, Greenberg PD. The use of anti-CD3 and anti-CD28 monoclonal antibodies to clone and expand human antigen-specific T cells. J Immunol Methods 1990;128:189–201.
29. Gillies SD, Reilly EB, Lo KM, Reisfeld RA. Antibody-targeted interleukin 2 stimulates T-cell killing of autologous tumor cells. Proc Natl Acad Sci U S A 1992;89:1428–32.
30. Cooper LJ, Al-Kadhimi Z, Serrano LM, et al. Enhanced antilymphoma efficacy of CD19-redirected influenza MP1-specific CTLs by cotransfer of T cells modified to present influenza MP1. Blood 2005;105: 1622–31.
31. Lupton SD, Brunton LL, Kalberg VA, Overell RW. Dominant positive and negative selection using a hygromycin phosphotransferase-thymidine kinase fusion gene. Mol Cell Biol 1991;11:3374–8.
32. Rentsch B, Bucher U, Brun del Re GP. Biochemical identification of the antigen recognized by the monoclonal pan-B cell antibody Y29/55. Eur J Haematol 1991; 47:204–12.
33. Treon SP, Mitsiades C, Mitsiades N, et al. Tumor cell expression of CD59 is associated with resistance to CD20 serotherapy in patients with B-cell malignancies. J Immunother 2001;24:263–71.
34. Foran JM, Rohatiner AZ, Cunningham D, et al. European phase II study of rituximab (chimeric

anti-CD20 monoclonal antibody) for patients with newly diagnosed mantle-cell lymphoma and previously treated mantle-cell lymphoma, immunocytoma, and small B-cell lymphocytic lymphoma. J Clin Oncol 2000;18:317–24.
35. Maloney DG, Grillo-Lopez AJ, White CA, et al. IDEC-C2B8 (Rituximab) anti-CD20 monoclonal antibody therapy in patients with relapsed low-grade non-Hodgkin's lymphoma. Blood 1997;90:2188–95.
36. Reff ME, Carner K, Chambers KS, et al. Depletion of B cells *in vivo* by a chimeric mouse human monoclonal antibody to CD20. Blood 1994;83:435–45.
37. McLaughlin P, Grillo-Lopez AJ, Link BK, et al. Rituximab chimeric anti-CD20 monoclonal antibody therapy for relapsed indolent lymphoma: half of patients respond to a four-dose treatment program. J Clin Oncol 1998;16:2825–33.
38. Lode HN, Reisfeld RA. Targeted cytokines for cancer immunotherapy. Immunol Res 2000;21:279–88.
39. Penichet ML, Morrison SL. Antibody-cytokine fusion proteins for the therapy of cancer. J Immunol Methods 2001;248:91–101.
40. Jurcic JG, Scheinberg DA. Recent developments in the radioimmunotherapy of cancer. Curr Opin Immunol 1994;6:715–21.
41. Kreitman RJ, Wilson WH, White JD, et al. Phase I trial of recombinant immunotoxin anti-Tac(Fv)-PE38 (LMB-2) in patients with hematologic malignancies. J Clin Oncol 2000;18:1622–36.
42. Pastan I. Targeted therapy of cancer with recombinant immunotoxins. Biochim Biophys Acta 1997; 1333:1–6.
43. Chianese-Bullock KA, Woodson EM, Tao H, et al. Autoimmune toxicities associated with the administration of antitumor vaccines and low-dose interleukin-2. J Immunother 2005;28:412–9.
44. Rosenberg SA, Lotze MT, Muul LM, et al. Observations on the systemic administration of autologous lymphokine-activated killer cells and recombinant interleukin-2 to patients with metastatic cancer. N Engl J Med 1985;313:1485–92.
45. Siegel JP, Puri RK. Interleukin-2 toxicity. J Clin Oncol 1991;9:694–704.
46. Gritzapis AD, Mamalaki A, Kretsovali A, et al. Redirecting mouse T hybridoma against human breast and ovarian carcinomas: *in vivo* activity against HER-2/neu expressing cancer cells. Br J Cancer 2003;88:1292–300.
47. Moritz D, Wels W, Mattern J, Groner B. Cytotoxic T lymphocytes with a grafted recognition specificity for ERBB2-expressing tumor cells. Proc Natl Acad Sci U S A 1994;91:4318–22.
48. Parker LL, Do MT, Westwood JA, et al. Expansion and characterization of T cells transduced with a chimeric receptor against ovarian cancer. Hum Gene Ther 2000; 11:2377–87.
49. Haynes NM, Snook MB, Trapani JA, et al. Redirecting mouse CTL against colon carcinoma: superior signaling efficacy of single-chain variable domain chimeras containing TCR-ζ vs Fc epsilon RI-γ. J Immunol 2001; 166:182–7.
50. Kahlon KS, Brown C, Cooper LJ, Raubitschek A, Forman SJ, Jensen MC. Specific recognition and killing of glioblastoma multiforme by interleukin 13-zetakine redirected cytolytic T cells. Cancer Res 2004;64:9160–6.

Redirecting Specificity of T-Cell Populations For CD19 Using the *Sleeping Beauty* System

Harjeet Singh,[1] Pallavi R. Manuri,[1] Simon Olivares,[1] Navid Dara,[1] Margaret J. Dawson,[1] Helen Huls,[1] Perry B. Hackett,[3] Donald B. Kohn,[4] Elizabeth J. Shpall,[2] Richard E. Champlin,[2] and Laurence J.N. Cooper[1]

Divisions of [1]Pediatrics and [2]Cancer Medicine, University of Texas M. D. Anderson Cancer Center, Houston, Texas; [3]Department of Genetics, Cell Biology and Development, University of Minnesota, St. Paul, Minnesota; and [4]Division of Research Immunology/Bone Marrow Transplantation, Children's Hospital Los Angeles, Los Angeles, California

Abstract

Genetic modification of clinical-grade T cells is undertaken to augment function, including redirecting specificity for desired antigen. We and others have introduced a chimeric antigen receptor (CAR) to enable T cells to recognize lineage-specific tumor antigen, such as CD19, and early-phase human trials are currently assessing safety and feasibility. However, a significant barrier to next-generation clinical studies is developing a suitable CAR expression vector capable of genetically modifying a broad population of T cells. Transduction of T cells is relatively efficient but it requires specialized manufacture of expensive clinical grade recombinant virus. Electrotransfer of naked DNA plasmid offers a cost-effective alternative approach, but the inefficiency of transgene integration mandates *ex vivo* selection under cytocidal concentrations of drug to enforce expression of selection genes to achieve clinically meaningful numbers of CAR$^+$ T cells. We report a new approach to efficiently generating T cells with redirected specificity, introducing DNA plasmids from the *Sleeping Beauty* transposon/transposase system to directly express a CD19-specific CAR in memory and effector T cells without drug selection. When coupled with numerical expansion on CD19$^+$ artificial antigen-presenting cells, this gene transfer method results in rapid outgrowth of CD4$^+$ and CD8$^+$ T cells expressing CAR to redirect specificity for CD19$^+$ tumor cells. [Cancer Res 2008;68(8):2961–71]

Introduction

The most robust example of successful T-cell therapy occurs following allogeneic hematopoietic stem-cell transplantation where the engrafted donor-derived T cells recognize recipient tumor-associated antigens in the context of MHC. However, the graft-versus-tumor effect after allogeneic-hematopoietic stem cell transplantation is incomplete, resulting in relapse as the major cause of mortality. To augment the graft-versus-tumor effect for B-lineage neoplasms, we have previously shown that genetically modified peripheral blood– and umbilical cord blood–derived T cells can be rendered specific for CD19, a molecule constitutively expressed on B-cell malignancies (1, 2). The redirected specificity was achieved by electrotransfer of a linearized DNA plasmid coding for a first-generation chimeric antigen receptor (CAR), designated CD19R, which recognizes CD19 via the scFv of a murine CD19-specific monoclonal antibody (mAb) fused to a chimeric CD3-ζ–derived activation endodomain. A phase I trial (BB-IND1141, clinicalTrials.gov identifier: NCT00182650; ref. 3) is currently evaluating the safety and feasibility of infusing autologous T cells electroporated to coexpress CD19R CAR and the hygromycin phosphotransferase (Hy) and herpes simplex virus-1 thymidine kinase selection/suicide fusion transgene (4).

We anticipated that the therapeutic efficacy of adoptive transfer of CD19-specific T cells would be improved by developing a CAR with a fully competent activation signal and introducing the CAR into central memory (CM) T cells. As a result, a second-generation CAR, designated CD19RCD28, has been developed that provides CD19-dependent signaling through chimeric CD3-ζ and CD28, resulting in improved *in vivo* persistence and antitumor effect, compared with CD19R$^+$ T cells (5). To further optimize the clinical potential of CAR$^+$ T cells, while taking advantage of the cost-efficiency of nonviral gene transfer, we desired a clinically feasible approach to the efficient propagation of CAR$^+$ T-cell populations, including T_{CM}, in the absence of expression immunogenic drug selection genes, such as *Hy*. We reasoned that genetically modified T cells could be selectively propagated, upon activating T cells for sustained proliferation, through the introduced second-generation CAR. To maximize transgene expression, we codon-optimized (CoOp) the CAR as reports have shown that codon optimization of genes toward human consensus codon usage increases protein expression (6, 7).

The focus on developing nonviral gene transfer technologies is justified based on the cost and time savings compared with developing recombinant clinical-grade viral supernatant, which are subject to rigorous regulatory oversight and rely on specialized manufacturing experience of a limited number of production facilities. Although the transfection efficiency of nonviral gene transfer is inferior to viral-mediated transduction, naked DNA plasmids expressing desired transgenes such as CAR can be rapidly produced at a fraction of the cost compared with clinical grade γ-retrovirus and lentivirus. A potential drawback to nonviral gene transfer, compared with viral gene transfer, is the lengthy *ex vivo* manufacturing time to selectively propagate electroporated T cells with stable expression of transgene, during which time the cells may become susceptible to replicative senescence, lose expression of desired homing receptors, and furthermore be cleared *in vivo* due to recognition of immunogenic drug selection transgene (8, 9). What is needed is an approach that when coupled with nonviral gene transfer shortens the culture time to generate T cells with durably expressed transgene and maintains a desired T-cell immunophenotype.

To introduce the CAR, we evaluated whether the efficient transposition and long-lasting transgene expression of the

Requests for reprints: Laurence J.N. Cooper, University of Texas M. D. Anderson Cancer Center, Pediatrics-Research, Unit 907, 1515 Holcombe Boulevard, Houston, TX 77030. Phone: 713-563-3208; Fax: 713-792-9832; E-mail: ljncooper@mdanderson.org.

doi:10.1158/0008-5472.CAN-07-5600

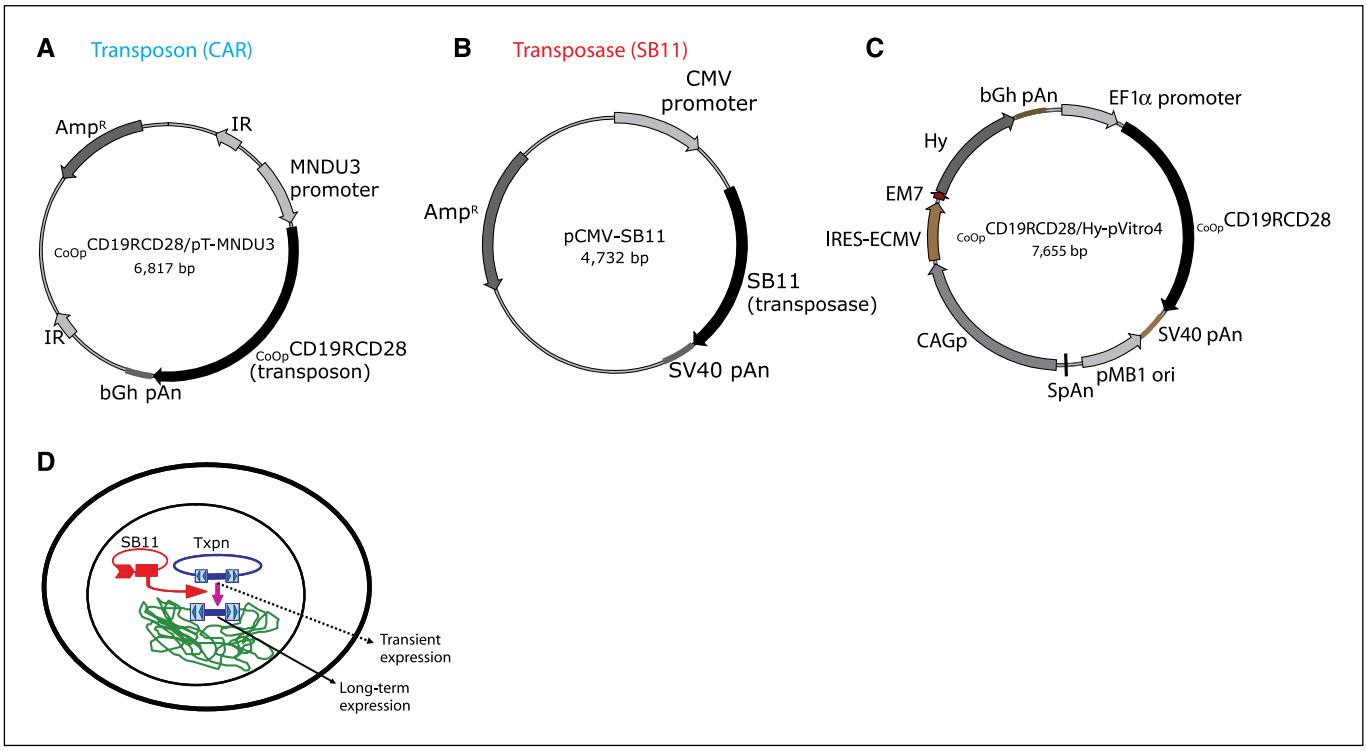

Figure 1. Schematic of the expression plasmids and experimental design. *A,* $_{CoOp}$CD19RCD28/pT-MNDU3 (*Transposon*). *MNDU3 promoter,* the constitutive promoter from the U3 region of the MND retrovirus; *$_{CoOp}$CD19RCD28,* codon-optimized CD19RCD28 CAR; *IR, SB*-inverted/direct repeats; *bGh pAn,* polyadenylation signal from bovine growth hormone; *Amp^R,* ampicillin resistance gene. *B,* pCMV-SB11 (*Transposase*). *SB11, SB*-transposase SB11; *CMV promoter,* CMV enhancer/promoter; *SV40pAN,* polyadenylation signals from SV40. *C,* $_{CoOp}$CD19CD28/Hy-pVitro4. *EF1α promoter,* composite promoter comprising the elongation factor-1α (*EF1α*) core promoter and the R segment and part of the U5 sequence (R-U5′) of the human T-cell leukemia virus type 1 LTR; *pMB1 ori,* a minimal *E. coli* origin of replication; *SpAn,* synthetic pause; *CAGp,* a composite promoter that combines the human CMV immediate-early enhancer and a modified chicken β-actin promoter and first intron; *Hy,* hygromycin B resistance gene (hygromycin phosphotransferase); *bGh pAn,* polyadenylation signal from bovine growth hormone; *EM7*, synthetic prokaryotic promoter. *D,* an expression cassette in a plasmid (*blue*) provides only transient expression unless incorporated into an integrating transposon vector that can be cleaved from the plasmid and integrated into a host genome by a source of transposase (*red*).

Sleeping Beauty (*SB*) DNA transposon derived from *Tc1/mariner* superfamily of transposons (10, 11) can improve transgene transfer efficiency. The *SB* transposable element from a DNA donor plasmid can be adapted for nonviral gene transfer in T cells, using a *SB* transposase supplied *in trans* to mediate integration of a transposon CAR expression cassette flanked by terminal inverted repeats (IR), which each contain two copies of a short direct repeat (DR) that have binding sites for the transposase enzyme (Fig. 1*D*). The *SB* transposase mediates transposition by binding to IRs, excising a precise DNA sequence flanked by the IRs, and inserting the transposon into any of ~200 million TA sites in a mammalian genome (12). Previously, the *SB* system has been used as a nonviral gene delivery into multiple murine and human cell lines, including liver, keratinocytes, endothelial cells, lung, hematopoietic progenitor cells, embryonic stem cells, and tumor cells (11). Of particular relevance is that *SB*-mediated integration has been shown in human T cells (13), signifying the potential application of this technology.

We report that electrotransfer of a two-component DNA *SB* system into primary human T cells from umbilical cord blood and peripheral blood results in efficient and stable CAR gene transfer, which can be numerically expanded to clinically meaningful numbers within 4 weeks on CD19$^+$ artificial antigen-presenting cell (aAPC), without the need for addition of cytocidal concentrations of drug for selection, and with the outgrowth of CD8$^+$ and CD4$^+$ CM and effector CAR$^+$ T-cell subpopulations. This was achieved through the rationale design of (*a*) a next-generation codon-optimized CD19-specific CAR, (*b*) CD19$^+$ aAPC expressing desired costimulatory and cytokine molecules, and (*c*) *SB* DNA plasmids expressing CAR transposon and an improved transposase. The relative ease of DNA plasmid production, electroporation, and outgrowth of stable integrants on a thawed γ-irradiated bank of aAPC can be readily transferred to the facilities operating in compliance with current good manufacturing practice (cGMP) for phase I/II trials. This is predicted to greatly facilitate trial design infusing CD4$^+$ and CD8$^+$ CAR$^+$ T cells that have desired immunophenotype, including T_{CM}.

Materials and Methods

Plasmids. The plasmid pT-MNDU3-eGFP containing salmonid fish–derived *SB* IR flanking the constitutive promoter, derived from the U3 region of the MND retrovirus (14), to drive an eGFP reporter gene (15), was derived from the plasmid pT-MCS (16) that was derived from pT/neo (10). The second-generation CD19RCD28 CAR (5) was human codon optimized (CoOp), substituting codons with those optimally used in mammals (GENEART) without altering anticipated amino acid sequence. The codon-optimized CD19RCD28 ($_{CoOp}$CD19RCD28) CAR was subcloned into pT-MNDU3 DNA plasmid by replacing the eGFP sequence with the CAR to create $_{CoOp}$CD19RCD28/pT-MNDU3 (Fig. 1*A*). The DNA plasmid pCMV-SB11 (Fig. 1*B*) expresses the SB11 transposase (17). Plasmid $_{CoOp}$CD19RCD28/Hy-pVitro4 (Fig. 1*C*) was generated from pVitro4-mcs DNA vector (InvivoGen) by subcloning $_{CoOp}$CD19RCD28 at *Nhe*I in multiple cloning site two and replacing the internal ribosome entry site (IRES) for the foot and mouth disease virus with that of the encephalomyocarditis virus (from pMG vector described; ref. 6). To

generate cell surface–bound human interleukin 15 (IL-15), the granulocyte macrophage colony-stimulating factor signal peptide sequence was fused to the coding sequence of mature human IL-15 at the 5′ end of a modified human IgG4 Fc region (5) fused in frame to human CD4 transmembrane domain and correct assembly was verified by DNA sequence analysis. The membrane-bound IL-15-Fc cytokine fusion gene was subcloned into pIRESpuro3 (Clontech) to obtain IL-15-Fc/pIRESpuro3.

Cell lines and primary human T cells. Daudi (Burkitt lymphoma) and HLA^{null} K562 (erythroleukemia) cells were obtained from American Type Culture Collection. Lymphoblastoid cells (LCL) were a kind gift of Dr. Helen Heslop (Cell and Gene Therapy, Baylor College of Medicine, Houston TX). These cell lines were cultured in HyQ RPMI 1640 (Hyclone) supplemented with 2 mmol/L Glutamax-1 (Life Technologies-Invitrogen) and 10% heat-inactivated defined FCS (Hyclone), referred to as culture medium (1). Human T cells were isolated by density gradient centrifugation over Ficoll-Paque-Plus (GE Healthcare Bio-Sciences AB), from umbilical cord blood or peripheral blood mononuclear cells (PBMC) after consent, and were cultured in culture medium.

Generation of aAPC. As previously reported, K562 cells were electroporated with DNA plasmids to enforce expression of all of the following: truncated CD19, 4-1BBL, and MICA fused to GFP (18). These aAPCs were further modified to express membrane-bound IL-15 to provide a cytokine stimulus at the site of CAR-binding and T-cell costimulation (19).

Electroporation and T-cell coculture with aAPC. On day 0, PBMCs and umbilical cord blood mononuclear cells (10^7) were suspended in 100 μL of Amaxa Nucleofector solution (CD34 kit) and mixed with 5 μg of supercoiled $_{CoOp}$CD19RCD28/pT-MNDU3 and 5 μg pCMV-SB11 DNA plasmids, transferred to a cuvette, and electroporated (Program U-14). After a 10-min room temperature incubation, the cells were transferred to a six-well plate containing 3 to 4 mL incomplete phenol-free RPMI and rested for 2 to 3 h. The cells were cultured overnight in 6 to 7 mL 10% phenol-free RPMI and stimulated the next day (day 1) with γ-irradiated (100 Gy) aAPC at a 1:10 T cell/aAPC ratio. The γ-irradiated aAPC were re-added every 7 d. Recombinant human interleukin 2 (rhIL-2; Chiron) was added to the cultures at 50 units/mL on a Monday-Wednesday-Friday schedule, beginning day 1 of each 7-d expansion cycle. The supercoiled plasmid $_{CoOp}$CD19RCD28/Hy-pVitro4 (expressing CAR under control of EF1α promoter and *Hy* under control of CAG promoter) was electroporated (10 μg) into PBMCs (10^7) using Nucleofector technology and T cells were propagated by cross-linking CD3 using an OKT3-mediated 14-d rapid expansion protocol (REP) as described previously using allogeneic γ-irradiated PBC and LCL feeder cells in the presence of exogenous (soluble) rhIL-2 (20). T cells were enumerated every 7 d, and viable cells were counted based on trypan blue exclusion.

Western blot. Expression of the chimeric 66-kD (CD19R) and 79-kD (CD19RCD28) CD3-ζ was accomplished using a primary mouse anti-human CD3-ζ mAb (1 μg/mL; BD Biosciences) and secondary horseradish peroxidase (HRP)–conjugated goat anti-mouse IgG (1:75,000; Pierce) under reducing conditions, based on methods previously described (20). Protein lysates were transferred onto nitrocellulose membrane using iBlot Dry Blotting System (Invitrogen) and developed with SuperSignal West Femto Maximum Sensitivity substrate (Pierce) per the manufacturer's instructions and chemiluminescence was captured after 1-min exposure using VersaDoc MP 4000 Imaging System (Bio-Rad).

Generation of monoclonal antibody recognizing a CD19-specific CAR. Female BALB/c mice were injected six times in the foot at 3-d intervals with syngeneic NS0 cells expressing CD19R CAR. Three days after the last immunization, mice were sacrificed, popliteal lymph nodes were removed, and cells were fused with P3-8AG-X653 myeloma cells at a ratio of 3:5, using 30% polyethylene glycol 1450 (in serum free RPMI containing 5% DMSO). After 10 d, hybridoma colonies were picked, cloned by limiting dilution in 96-well plates, and 100 μL of supernatants were screened by ELISA for differential binding to round-bottomed 96-plates containing adsorbed (10^5/well) $CD19R^+$ and $CD19R^{neg}$ Jurkat cells as detected by 1:500 dilution of HRP-conjugated goat anti-mouse IgG (Santa Cruz Biotechnology). Detection was achieved by TMB Microwell peroxidase substrate system (KPL). Protein G column (Roche) purified mAb was conjugated to Alexa Fluor 488 (Invitrogen-Molecular Probes) per manufacturer's instructions.

Flow cytometry. Fluorochrome-conjugated reagents were obtained from BD Biosciences: anti-CD4, anti-CD8, anti-CD25, anti-CD27, anti-CD28, anti-CD62L, anti-CD45RA, anti-CD45RO, and anti-CD95. Affinity-purified $F(ab')_2$ fragment of FITC-conjugated goat anti-human Fcγ (Jackson Immunoresearch) was used at 1/20 dilution to detect cell surface expression of CD19-specific CAR. Purified CAR-specific mAb clone 2D3, conjugated to Alexa Fluor 488, was used at a dilution of 1/30, giving a concentration of ~30 μg/mL. In some experiments, binding of this mAb to the Fc region of CAR was blocked (30 min at 4°C) using goat human Fc-specific antiserum (Sigma). Blocking of nonspecific antibody binding was achieved using FACS wash buffer (2% FCS in PBS). T-cell receptor (TCR)-Vβ expression was determined with a panel of 24 TCR-Vβ–specific mAbs (IO TEST Beta Mark TCR-Vβ repertoire kit, Beckman Coulter) used in association with anti-CD3 and appropriate isotype-matched control mAbs. Data acquisition was on a FACSCalibur (BD Biosciences) using CellQuest version 3.3 (BD Biosciences). Analyses and calculation of mean fluorescence intensity (MFI) was undertaken using FCS Express version 3.00.007 (Thornhill).

Intracellular IL-2 cytokine staining. Intracellular IL-2 was assayed using the Intracellular Cytokine Staining Starter Kit (BD PharMingen) per the manufacturer's instructions. Briefly, 10^5 T cells were incubated with 0.5×10^6 stimulator cells in 200 μL culture medium along with protein transport inhibitor (BD Golgi Plug containing Brefeldin A) in a 96-well plate. Following a 4- to 6-h incubation at 37°C, the cells were stained for CAR expression using hybridoma mAb clone 2D3 at 4°C for 30 min. After washing, the cells were fixed and permeabilized (100 μL, Cytofix/Cytoperm buffer) and phycoerythrin-conjugated mAb specific for IL-2 was added. Cells were further washed and analyzed by FACSCalibur. T cells were treated with a leukocyte activation cocktail (phorbol 12-myristate 13-acetate and ionomycin) as a positive control.

Confocal microscopy. Jurkat parental and $CD19R^+$ Jurkat cells were stained with the hybridoma clone mAb 2D3, at a 1:50 dilution for 15 min at 4°C, washed in FACS wash buffer, and fixed with 0.1% paraformaldehyde. After fixing, the cells were washed twice with FACS wash buffer and transferred onto slides, and coverslips were mounted with Prolong Gold anti-fade agent (Invitrogen). Cells were examined under a confocal microscope (Leica TCS SP2-SE) using oil immersion lens (×63 objective). Single-scan images were obtained with a 4.76× zoom in a 1,024 × 1,024 format with a line averaging of 8.

Chromium release assay. The cytolytic activity of T cells was determined by 4-h chromium release assay (1). CD19-specific T cells were incubated with 5×10^3 ^{51}Cr-labeled target cells in a V-bottomed 96-well plate (Costar). The percentage of specific cytolysis was calculated from the release of ^{51}Cr, as described earlier, using a TopCount NXT (Perkin-Elmer Life and Analytical Sciences, Inc.). Data are reported as mean ± SD.

DNA PCR for *SB* transposon and transposase. DNA was isolated from PBMC using the QIAmp DNA mini kit (Qiagen). PCR was carried out using CD19RCD28-specific forward primer 5′-AGATGACCCAGACCACCTCCAGC-3′ and reverse primer 5′-GGTATCCTTGGTGGCGGTGCT-3′ for the transposon. The PCR reaction used 1 μg of DNA/sample in a mix containing 10× PCR buffer, 2.5 mmol/L deoxynucleotide triphosphates, 3 μmol/L $MgCl_2$, and 0.5 units of DNA polymerase (AmpliTaq Gold, Applied Biosystems) in a final volume of 50 μL amplified in a thermal Cycler (PTC-200 DNA Engine Cycler, Bio-Rad). After an initial denaturation at 95°C for 5 min, the samples underwent 34 cycles of 95°C for 30 s, 65°C for 30 s, 72°C for 1 min 15 s, followed by a prolonged extension step at 72°C for 7 min. For the transposase gene, PCR was carried out using SB11-specific forward primer 5′-ATGGGACCACGCAGCCG-3′ and reverse primer 5′-CGTTTCGGGTAGCCTTCCACA-3′. After an initial denaturation at 95°C for 5 min, the samples underwent 34 cycles of 95°C for 15 s, 58°C for 30 s, 74°C for 2 min followed by a prolonged extension step at 74°C for 7 min. The housekeeping gene *GAPDH* was also amplified in the same samples using the forward primer 5′-TCTCCAGAACATCATCCCTGCCAC-3′ and reverse primer 5′-TGGGCCATGAGGTCCACCACCCTG-3′.

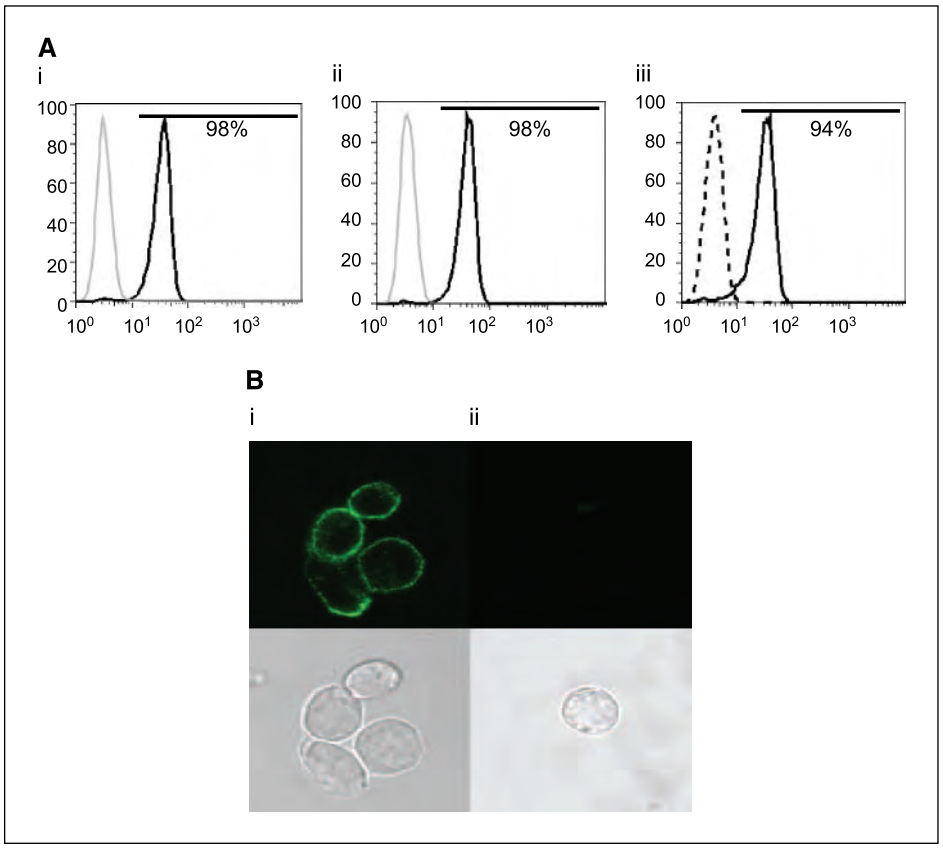

Figure 2. Specificity of mouse-derived CAR-specific mAb (clone 2D3). *A,* Jurkat cells were genetically modified and sorted to express CD19R. Jurkat parental (*gray line*) and CD19R$^+$ (*black line*) cells were stained with (*i*) Alexa 488–conjugated clone 2D3 and (*ii*) F(ab′)$_2$-fragment of goat-derived polyclonal antibody specific for human Fc; *iii,* binding of 2D3 (*solid line*) was blocked by polyclonal Fc-specific antisera (*dashed line*). *B,* cell surface staining of Alexa Fluor 488–conjugated clone 2D3 by confocal microscopy on (*i*) CD19R$^+$ Jurkat cells and (*ii*) Jurkat parental cells. Cells were stained, fixed, and mounted as described in Materials and Methods.

Chromosome banding analysis. Exponentially growing *SB*-transfected T-cell cultures (freshly fed 24 h earlier) were incubated for 2 h at 37°C with colcemid (20 μL of 0.04 μg/mL) per 10 mL medium followed by 0.075 mol/L KCl at room temperature for 15 min, fixed with acetic acid/methanol (1:3), and washed thrice on a glass slide. For Giemsa (G) banding, 5- to 6-d-old slides treated with trypsin were stained with Giemsa stain following standard techniques described previously (21). A total of 15 G-banded metaphases were photographed and 5 complete karyotypes were prepared using a karyotyping system from Applied Imaging Corporation.

Results

We describe a new approach to using nonviral gene transfer of DNA plasmids to efficiently obtain populations of memory and effector T cells with desired specificity (Fig. 1*D*). The system we have devised provides for robust antigen-driven expansion of CD4$^+$ and CD8$^+$ CAR$^+$ T cells to clinically meaningful numbers.

Monoclonal antibody with specificity for CD19-specific CAR. The cell surface expression of the introduced CAR was predicted to increase with outgrowth of T-cell populations that have undergone CAR-mediated numerical expansion on CD19$^+$ aAPC. Currently, the only-commercially available flow cytometry reagents that recognize our CARs are polyclonal anti-Fc antibodies raised in goat, but we desired a homogeneous monoclonal product for use in the release of CAR$^+$ T cells for clinical trials. To longitudinally follow the transgene expression, we developed a CAR-specific mAb by immunizing mice with syngeneic NS0 cells expressing CD19R. A hybridoma mAb clone 2D3 (IgG1) was selected by flow cytometry that selectively bound to CD19R$^+$ Jurkat cells, but not parental Jurkat cells. The binding of 2D3 can be blocked using a Fc-specific antibody (Fig. 2*A*). The 2D3 clone bound a CD20-specific CAR that shares the IgG4 Fc region with CD19R and CD19RCD28 (data not shown). The pattern of staining by confocal microscopy showed 2D3 binding to CAR on the cell surface (Fig. 2*B*). These data are consistent with a mAb binding specifically to the CD19-specific CAR and recognizing the modified human IgG Fc region. Of note, the production of this mAb avoided the need to purity recombinant CAR protein as the immunogen was genetically modified NS0 cells and the ELISA screening used genetically modified Jurkat cells.

Electrotransfer of *SB* two-plasmid DNA system. We have used a nonviral gene transfer approach to introduce codon optimized DNA expression plasmids because these expression vectors can be readily and cheaply manufactured to clinical grade. Although codon modification of TCR genes has been shown to enhance expression of transgenic TCR in primary human T cells (22), we now show the usage of a codon optimized second-generation CAR. Previously, our electroporation approach based on the Multiporator (Eppendorf; refs. 23, 24) used T cells that had been stimulated to proliferate by cross-linking CD3 with OKT3 to allow access of the introduced naked DNA to the nucleus after dissolution of the nuclear envelope during prometaphase. However, T cells nonspecially activated to proliferate, such as by cross-linking CD3 as occurs in the REP (25), would preclude subsequent immediate antigen-mediated propagation and thus directed outgrowth of CAR$^+$ T cells. Nucleofector technology has been used to electroporate nonreplicating cells by direct transfer of DNA to the nucleus (26). Thus, we investigated whether this electrotransfer system could be used to genetically modify circulating T cells from peripheral blood and umbilical cord blood, which are in a

Table 1. Percent CAR expression in T cells after electroporation of CAR transposon with or without SB11 transposase plasmid

DNA plasmid(s)	Day 1						Day 28					
	$CD4^+CAR^+$		$CD8^+CAR^+$		Total CAR^+		$CD4^+CAR^+$		$CD8^+CAR^+$		Total CAR^+	
	PBMC	UCB	PBMC	UCB	PBMC	UCB	PBMC	UCB	PBMC	UCB	PBMC	UCB
No DNA	0.6	1.0	0.2	0.1	1.6	1.3						
SB11	0.9	1.1	0.8	0.2	1.2	1.4						
Txpn*	15.9	10.7	9.5	1.0	27.0	11.8	0.07	0.8	0.5	0.3	0.8	3.5
Txpn* and SB11	13.3	4.9	7.9	0.8	22.0	5.4	27.5	24.8	13.5	1.9	38.9 †	29.7 ‡

Abbreviation: UCB, umbilical cord blood.

*Txpn (transposon) = $_{CoOp}$CD19RCD28/pT-MNDU3.

† When *SB* transposase is electroporated with transposon, there is 49-fold improved CAR expression.

‡ When *SB* transposase is electroporated with transposon, there is 8.4-fold improved CAR expression.

quiescent state. To assist with subsequent translation to clinical practice, the Nucleofector solution is available for use in cGMP.

Both the *SB* transposase and IR have been independently manipulated to improve efficiency of transposition, but changes to both do not generally seem to be additive. In preliminary experiments, we too compared the relative transposition efficiency of the SB10 (10, 16) and SB11 transposases (the latter exhibiting improved enzymatic activity; ref. 17) in a two-by-two matrix using the Amaxa 96-well Shuttle system to introduce these transposases and pT (15, 16) and pT2 transposons (the latter exhibiting improved transposition; ref. 27) into Jurkat T cells. As observed with other cell lines, we found a similar increase in transposition using SB11 with pT and using SB10 with pT2 (27) although, as reported, overproduction of transposase inhibited transposition (13, 17). When the pT2-improved transposon was combined with SB11, no further increase in transgene expression was observed over that achieved when these components were used with SB10 or pT, respectively. In the present study, a combination of pT transposon (for integration) and SB11 transposase (for transient expression) was used for experiments with primary T cells.

Generation of $CD19^+$ aAPC. We determined whether peripheral blood and umbilical cord blood–derived T cells could be selectively propagated by stimulating through an introduced immunoreceptor. This experiment would evaluate our underlying hypothesis of whether the presence of the *SB* transposase would improve efficiency of CAR transposon integration in T cells. Our initial attempts at CAR-dependent T-cell propagation after electrotransfer of the *SB* system used allogeneic LCL because these are widely available as master cell banks (including at M. D. Anderson Cancer Center) manufactured in compliance with cGMP for phase I/II trials. However, these LCL resulted in nonspecific outgrowth of CAR^{null} T cells that had undergone electrotransfer of *SB* plasmids, independent of CAR expression (data not shown), presumably due to outgrowth of alloreactive T cells. Because our *SB* transposon by design does not include a drug resistance gene, we avoided nonspecific propagation of T cells using K562 as aAPC because these do not express classical HLA molecules. K562 cells are widely recognized as a platform suitable for the numerical expansion of lymphocytes because they (*a*) can be cultured in compliance with cGMP, (*b*) express desired endogenous T-cell costimulatory molecules, (*c*) secrete pro-inflammatory cytokines, and (*d*) can be readily modified to enforce the expression of antigen and desired endogenous T-cell costimulatory molecules (28, 29). To provide an IL-15–mediated growth stimulus coordinated with recognition of CD19 antigen, the aAPC expressing tCD19, 4-1BBL, and MICA were further modified to express the IL-15 cytokine on the cell surface (IL-15-Fc; Fig. 2*A*). Membrane-bound IL-15 has been used before to propagate natural killer (NK) cells on K562 (19). The ability of these K562 aAPCs to propagate CAR^+ T cells after electrotransfer of *SB* transposon and transposase plasmids is described in the next section.

***SB*-mediated gene transfer of CAR transposon in primary T cells.** After using the Nucleofector to import plasmid DNA into quiescent T cells, we observed that peripheral blood– and umbilical cord blood–derived electroporated $CD4^+$ and $CD8^+$ T cells readily expressed the CAR transposon (Table 1; Fig. 3*A*). Not surprisingly, the presence of the plasmid expressing the SB11 transposase did not increase transposon expression when measured 24 hours after electroporation (22% and 27% CAR expression with and without transposase, respectively), as this early time point for assessing transgene expression records transient nonintegrated CAR expression (Fig. 3*A*). The genotoxicity reported with excess expression of *SB* transposase (17) was apparently controlled in our two-plasmid system using a 1:1 ratio of transposon and transposase. To obtain peripheral blood– and umbilical cord blood–derived T cells with integrated transposon, the genetically modified cells were cocultured with γ-radiated aAPC (K562 genetically modified to express tCD19, 4-1BBL, MICA, IL-15-Fc) at a ratio of 1:10 (T cell to aAPC). After 5 weeks of continuous coculture (γ-radiated aAPC re-added every 7 days), the percentage of peripheral blood–derived T cells expressing CAR increased in the transposase-containing group (43%), whereas the CAR expression was lost (0.7%) when transposon was electrotransferred in the absence of transposase (Fig. 3*A*). Thus, after 28 to 35 days, the efficiency of two DNA plasmid *SB*-mediated gene transfer improved CAR expression by ~49 to 60-fold, compared with a single plasmid transposon control (Table 1). The expression of the CAR was confirmed by Western blot of whole-cell lysates of propagated T cells probed using a mAb specific for CD3-ζ chain revealed the 79-kDa chimeric ζ chain in addition to the 21-kDa endogenous ζ chain (Fig. 3*C*). To monitor for the presence or absence of the integrated CD19RCD28 transgene, DNA from the

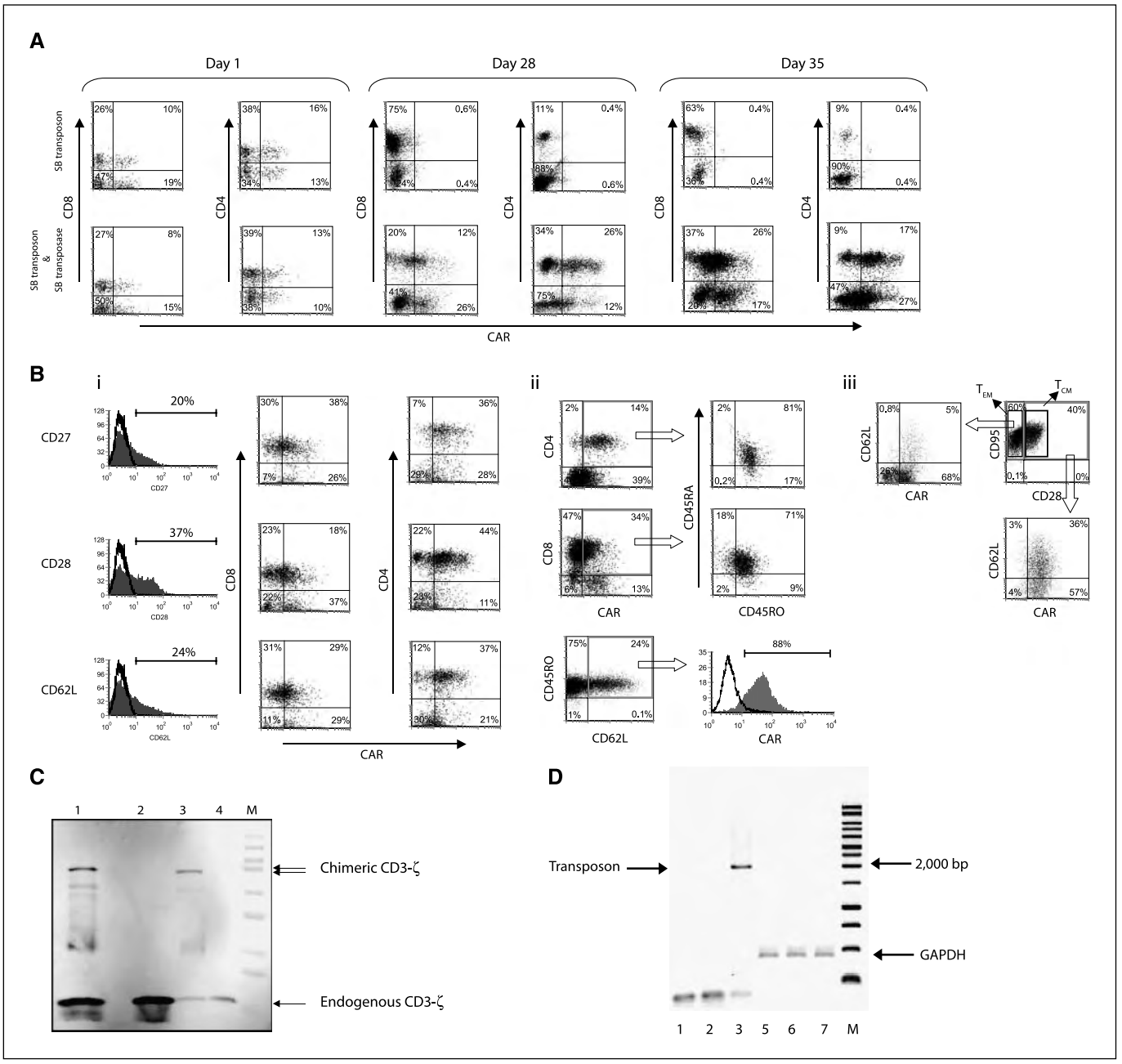

Figure 3. Characterization of CAR expression on peripheral blood–derived T cells after electrotransfer of *SB* plasmid system. *A,* expression of CAR on $CD8^+$ and $CD4^+$ T cells after electrotransfer of *SB* transposon with or without SB11 transposase at 24 h, and 4 and 5 wk of coculture on γ-irradiated K562-derived aAPC expressing tCD19, IL-15-Fc, MICA, and 4-1BBL. *B, i,* immunophenotype of memory cell markers (CD27, CD28, CD62L) on genetically modified T cells generated after 5 wk of coculture on aAPC. The gray-filled histograms reveal the percentage of T cells expressing CD27, CD28, and CD62L in the lymphocyte-gated population. Those expressing the memory cell markers were analyzed for coexpression of CAR (detected by mAb clone 2D3) and CD8 or CD4. *ii,* expression of CD45RO, CD45RA, and CD62L on T cells generated after coculture. CAR^+ CD4 or CD8 cells were analyzed for the expression of CD45RA and CD45RO. The MFI of the unmanipulated T cells was 867/50 (CD45RA/CD45RO) compared with 28/38 for the SB-transfected T cells. CD45RO and CD62L double-positive cells were also analyzed for coexpression of CAR. *iii,* T_{CM}, defined as double-positive for CD28 and CD95 (T_{EM}, $CD28^{neg}CD95^{pos}$), were analyzed for coexpression of CD62L and CAR. *C,* Western blot analysis of CAR expression detected by mAb specific for CD3-ζ. Whole-cell protein (20 μg) lysates from primary T cells genetically modified with $_{CoOp}$CD19RCD28 (*lane 1,* ~79 kDa chimeric protein) or no plasmid control (*lane 2*); $CD19R^+$ Jurkat cells (*lane 3,* ~66 kDa chimeric protein) or parental Jurkat (*lane 4*) were resolved by SDS-PAGE under reducing conditions. *D,* integration of $_{CoOp}$CD19RCD28 by PCR. DNA was isolated from T cells after mock electroporation (no DNA, *lanes 1* and *4*), from T cells 28 d after electroporation with *SB* transposon in the absence of transposase (*lanes 2* and *5*), and from T cells 28 d after electroporation with transposon in the presence of SB11 transposase (*lanes 3* and *6*). PCR was accomplished using transposon-specific primers (*lanes 1–3*) or GAPDH-specific primers (*lanes 4–6*). The data showing *SB* system in peripheral blood/cord blood are from a representative experiment.

numerically expanded T cells, electroporated with and without SB11, were PCR amplified using CAR-specific primers. A 1,900-bp band corresponding to the CD19RCD28 transgene was observed in T cells electroporated using the *SB* two-plasmid system, whereas no similar band was observed in cells electroporated with *SB* transposon in the absence of transposase, which is consistent with improved SB11-mediated transposition in T cells expressing CAR protein (Fig. 3*D*).

Propagation of CAR$^+$ T cells. The K562-derived aAPC was calculated to give a 20-fold growth of genetically modified T cells at the end of 4 weeks with continued and accelerated expansion thereafter (Fig. 4*A*). A subset analysis revealed that populations of both CD4$^+$CAR$^+$ and CD8$^+$CAR$^+$ T cells could be propagated (Table 1). Initially, the rates of CD4$^+$ and CD8$^+$ T-cell growth on aAPC were similar, but after ~8 weeks there was an outgrowth of CD4$^+$CAR$^+$ T cells (Fig. 4*B*). Thus, continued time in tissue culture could be used to derive CAR$^+$ T cells with an increased CD4 to CD8 ratio. We also followed the percentage expression and density of the CAR on the T-cell surface by flow cytometry. With coculture, there was outgrowth of percentage of T cells expressing the CD19-specific CAR (22% on day 1 and peaking at 99% on day 70). However, as the percentage of CAR$^+$ T cells increased, there was a decrease in the density of CAR expression, as the MFI dropped from a peak of 109 arbitrary units at 21 days, early in the coculturing process, and then declined over culture time. The amount of CAR for the population peaked at ~70 days after electroporation (percentage expression multiplied by MFI). Thus, adding a fixed ratio of aAPC (with a fixed density of CD19 antigen) to T cells seems to have supported the growth for populations of T cells that either expressed high density of CAR or high percentage of CAR.

Immunophenotype of CAR$^+$ memory T cells. Previously, T cells from healthy donors electroporated to express a CD19-specific CAR and nonspecifically activated for proliferation by cross-linking CD3 with OKT3 using REP have shown a predominant phenotype consistent with differentiated effector CD8$^+$ T cells (20). In contrast, after electrotransfer of *SB* plasmids and numerical expansion on aAPC, T cells exhibited a heterogeneous immunophenotype and apparently included populations of CAR$^+$ T_{CM}. We showed that the CAR$^+$ T cells expressed memory cell markers (CD27, CD28, CD62L; refs. 30–32) as well as determinants of an effector-cell phenotype (Fig. 3*Bi*). For example, over half of CD27$^+$, CD28$^+$, and CD62L$^+$ T cells expressed CAR. Indeed, as a marker for T_{CM}, 88% of the CD62L$^+$CD45RO$^+$ cells expressed the CAR (Fig. 3*Bii*; ref. 33). Upon

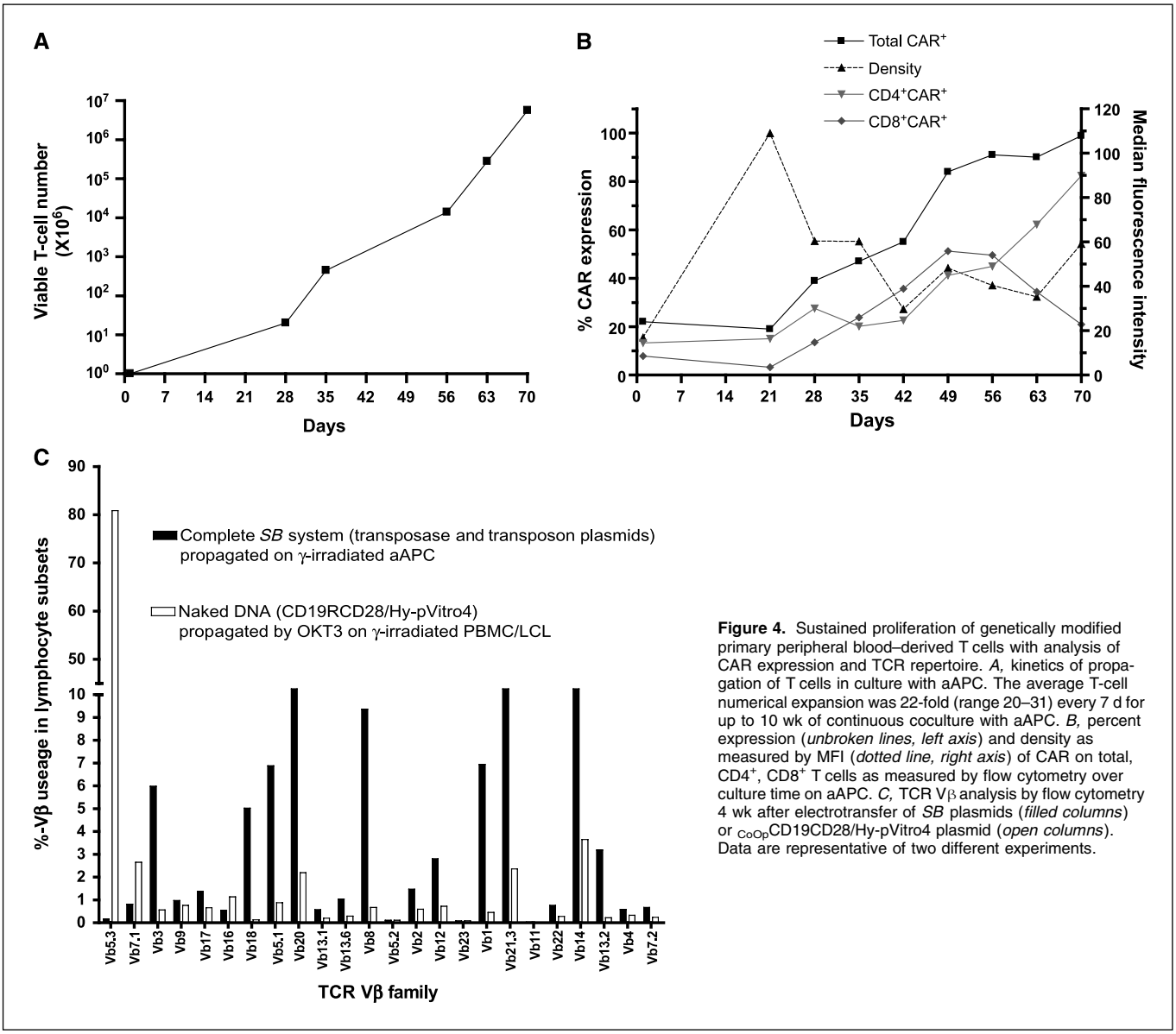

Figure 4. Sustained proliferation of genetically modified primary peripheral blood–derived T cells with analysis of CAR expression and TCR repertoire. *A,* kinetics of propagation of T cells in culture with aAPC. The average T-cell numerical expansion was 22-fold (range 20–31) every 7 d for up to 10 wk of continuous coculture with aAPC. *B,* percent expression (*unbroken lines, left axis*) and density as measured by MFI (*dotted line, right axis*) of CAR on total, CD4$^+$, CD8$^+$ T cells as measured by flow cytometry over culture time on aAPC. *C,* TCR Vβ analysis by flow cytometry 4 wk after electrotransfer of *SB* plasmids (*filled columns*) or $_{CoOp}$CD19CD28/Hy-pVitro4 plasmid (*open columns*). Data are representative of two different experiments.

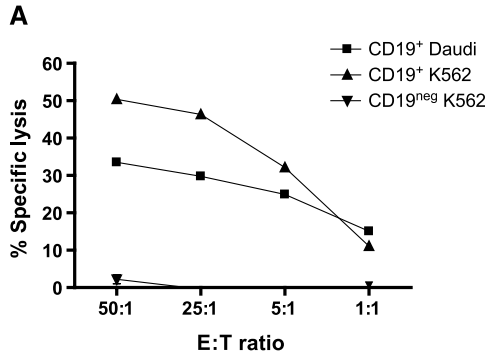

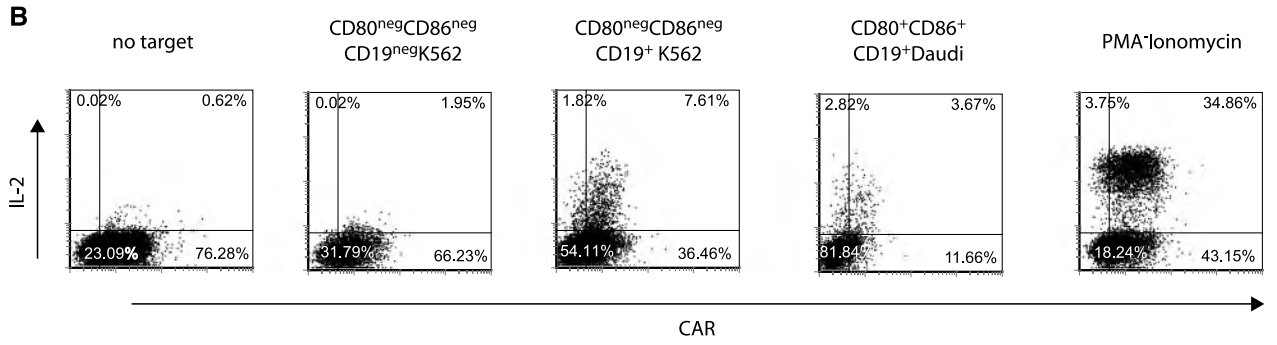

Figure 5. Redirected specificity of peripheral blood–derived T cells genetically modified with *SB* system. *A,* killing of $CD19^+$ target cells (HLA I^{neg} Daudi; HLA class I/II^{neg} K562 cells transfected to express truncated CD19) in a standard 4-h chromium release assay. Background lysis of $CD19^{neg}$ (parental K562) cells is shown. *Points,* mean specific lysis of triplicate wells at effector to target (*E:T*) cell ratios; *bars,* SD. *B,* CAR and intracellular IL-2 expression after incubating with panel of stimulator cells by multiparameter flow cytometry gating on $CD3^+$ lymphocytes. Phorbol 12-myristate 13-acetate (*PMA*) and ionomycin were added as a positive control.

gating $CD45RO^+$ cells, we observed a preferential expansion of T cells with this memory-cell marker in the cultured *SB*-transfected T cells (90%; MFI, 38) compared with unmanipulated T cells obtained directly from PBMC (36%; MFI, 50). T_{EM} and T_{CM} have also been distinguished based on relative expression of CD28 and Fas (34). Using these markers, we were able to identify that genetically modified and propagated T_{CM} constituted ~40% of the total cell population and $CD28^{neg}CD95^+$ T_{EM} represented the remainder of the propagated T cells. Multiparameter flow cytometry further revealed that 39% of $CAR^+CD28^+CD95^+$ T_{CM} expressed CD62L. In comparison, only 7% of the CAR^+ T_{EM} expressed CD62L (Fig. 3*Biii*). These data reveal that CAR^+ T cells are present in T cells that express markers consistent with T_{CM}. Preferential expansion of T cells in tissue culture with an apparent memory phenotype can also be inferred by from the ratio of CD45RA/CD45RO, which decreased from 2.75 in unmanipulated freshly derived PBMC to 0.9 for SB-transfected and *ex vivo* propagated T cells (Fig. 3*Bii*). The relative percentage increase of observed $CD45RO^+$ cells, or the decrease in CD45RA/CD45RO ratio, is presumably due to the repetitive antigenic stimulation of cultured T cells resulting in down-regulation of the high molecular weight CD45RA isoform and reciprocal up-regulation of the low molecular weight isoform CD45RO during time in culture. Coexpression of both CD45RA and CD45RO has been associated with the phenotype of effector T cells (35) but as in circulating peripheral blood–derived T cells express both CD45RA and CD45RO, the markers are presumably also present on memory cells. These data have implications for improved *in vivo* efficacy as T_{CM} are associated with long-term persistence after adoptive transfer.

TCR Vβ repertoire. We tracked the expression of TCR Vβ usage by flow cytometry over time with the hypothesis that an improvement in DNA-plasmid integration would be reflected by maintenance of a broad pre-electroporation TCR Vβ repertoire. The pattern of TCR Vβ usage observed after electrotransfer of the two DNA *SB* plasmids and propagation on aAPC was much broader than when T cells were electroporated using the single $_{CoOp}$CD19RCD28/Hy-pVitro4 plasmid and expanded by REP by cross-linking CD3 with OKT3 in cytocidal concentrations of hygromycin B. We observed that ~80% of the T cells electroporated with $_{CoOp}$CD19RCD28/Hy-pVitro4 plasmid expressed a single TCR Vβ family (Vβ5.3). In contrast, ~80% of the T cells electroporated with the complete *SB* system expressed 30% of the TCR Vβ families (Fig. 4*C*). This is consistent with less efficient integration of the $_{CoOp}$CD19RCD28/Hy-pVitro4 plasmid compared with the *SB* system. These data have implications for design of adoptive immunotherapy trials as maintaining a broad TCR diversity is desired to restore immune reconstitution after myeloablative preparative regimens.

Redirected function of CAR^+ T cells after electrotransfer of *SB* plasmids. The numerically expanded T cells were evaluated for redirected killing. The genetically modified T cells were able to lyse $CD19^+$ targets, and specificity of killing was shown by the background lysis of $CD19^{neg}$ K562 cells (Fig. 5*A*). We showed a 25-fold increase in specific lysis of $CD19^+$ K562 at effector-to-target ration of 50:1. The lack of killing of $CD19^{neg}$ K562 is consistent with absence of resident NK cell function in the culture, as these target cells are sensitive to NK cell–mediated lysis. Because the CAR contains a CD28 endodomain, we investigated whether T cell–derived IL-2 could be produced when CAR contacted CD19 antigen in the absence of binding CD80 or CD86. An intracellular cytokine assay showed that IL-2 could be detected in the CAR^+ T cells only when cultured with $CD19^+$ stimulator cells and not with $CD19^{neg}$ cells (Fig. 5*B*). There was an ~4-fold increase in IL-2 expression when CAR^+ T cells were stimulated by $CD19^+CD80^{neg}CD86^{neg}$ K562 cells compared with $CD19^{neg}$ K562 parental controls. No significant

IL-2 production was observed when T cells were cultured in absence of stimulator cells. These data are consistent with activation of T cells for killing and IL-2 cytokine production through the CAR.

Lack of integration of SB11 transposase in propagated T cells. Continued presence of the SB11 transposase in genetically modified T cells may cause genotoxicity. We evaluated for the presence of integrated transposase plasmid by genomic PCR. No band corresponding to the SB11 transposase gene (size ~830 bp) was detected in T cells that were electroporated with the *SB* transposon and transposase and had undergone 4 weeks of coculture with aAPC (Fig. 6*A*), which is consistent with the rapid loss of transposase expression activity over the first few days postdelivery in mice (36). These results indicate that the SB11 transposase was not integrated into the genome of cells stably expressing the CD19RCD28 CAR.

Karyotype of genetically modified T cells. As a measure of global genotoxicity associated with undesired and continued transposition, we evaluated the integrity of the chromosome structure. G-banding analysis of the *SB*-transfected T cells showed a normal female karyotype, 46, XX with no apparent numerical or structural chromosome alterations (Fig. 6*B*). Although this does not exclude chromosomal damage below the limit of detection of this technique, it supports the premise that *SB* transposition in T cells is not associated with translocations and chromosomal aberrations.

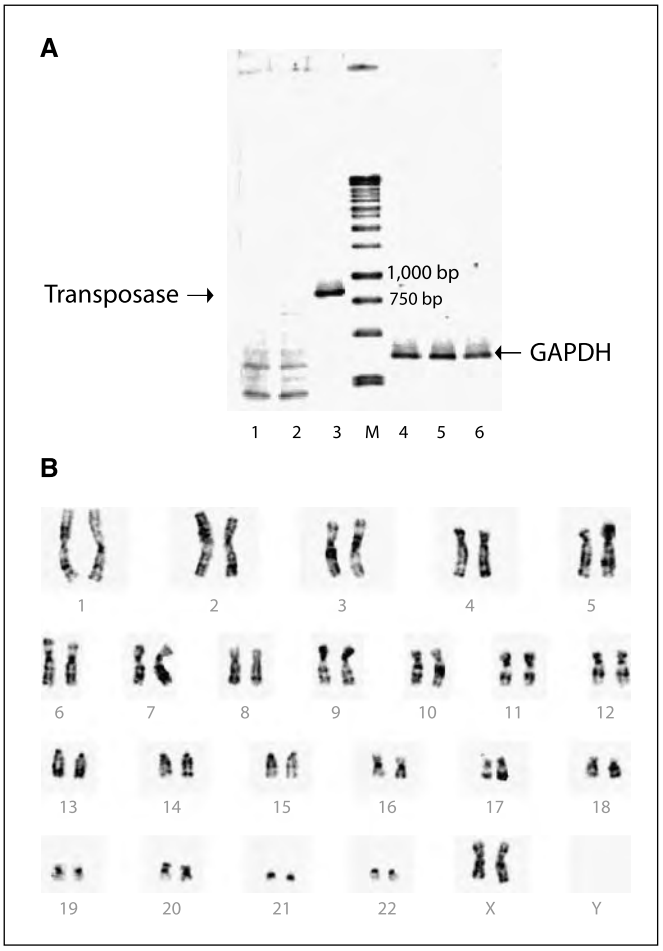

Figure 6. Safety issues regarding SB transposase and chromosomal aberrations. *A,* lack of integration of SB11 transposase by genomic PCR from genetically modified and propagated peripheral blood–derived T cells. DNA was isolated from T cells after mock electroporation (no DNA, *lanes 1* and *4*), from T cells 28 d after electroporation with the two-plasmid *SB* system (*lanes 2* and *5*), or from T cells 1 d after electroporation with the two-plasmid *SB* system (*lanes 3* and *6*). PCR was accomplished using transposase-specific primers (*lanes 1–3*) or GAPDH-specific primers (*lanes 4–6*). *B,* idiogram of a G-banded karyotype of the *SB*-transfected peripheral blood–derived T cells showing no apparent numerical or structural chromosome alterations.

Discussion

We have previously showed that peripheral blood– and umbilical cord blood–derived T cells can be rendered specific for CD19, based on using a CAR capable of providing a fully competent activation signal, development of aAPC-expressing antigen, and desired costimulatory signals. In this report, we describe the use of *SB* transposon/transposase plasmids to introduce CD19-specific CAR leading to efficient outgrowth of CAR^+ T cells on aAPC with preservation of $CD4^+$, $CD8^+$, central memory, and effector-cell immunophenotypes. This is expected to be of widespread interest as many institutions are evaluating the clinical potential of genetically modified T cells with redirected specificity. The majority of these programs use recombinant viral vectors, which, although efficient at gene transfer, are generally cost-prohibitive to manufacture to clinical grade and still permit incremental changes to clinical trial design. Yet, at this early stage of gene therapy planning with clinical grade T cells, what is needed, and is provided here, is a cost-effective gene transfer system that encourages reiterative changes to expression vector and/or CAR design to be used in proof-of-concept clinical trials that support hypothesis testing from the bench to the bedside and back again. The approximate cost for manufacture and release of a clinical grade plasmid DNA is between $20,000 and $40,000 depending on supplier and degree of release testing needed. This release testing typically requires restriction enzyme analyses, sequencing, and measures of (*a*) homogeneity/purity/contamination (protein, RNA, and other DNA) and (*b*) sterility including endotoxin. For early-phase proof-of-concept trials, this pricing compares favorably with the relatively high cost of recombinant retrovirus, including lentivirus as manufacture and release of clinical grade viruses may exceed 10 times the cost of DNA-plasmid production. Furthermore, there is downward pressure on the unit cost for DNA because there are many vendors worldwide with the capability to produce clinical grade plasmids. The manufacture/release of recombinant retrovirus is highly specialized, requiring the expertise of a small number of GMP facilities that contributes to high cost and can introduce delays to production and thus availability for clinical use.

Previously, the relatively low levels of nonviral gene transfer efficiency to introduce naked DNA plasmid coding CAR transgene, compared with viral-mediated transduction, has been compensated by lengthy periods of *ex vivo* tissue culture to select-out T cells expressing drug-metabolizing enzymes. Thus, an attractive feature of the *SB* gene transfer system to introduce CAR into T cells is avoidance of the need to express immunogenic section genes, such as bacteria-derived *Hy* transgene. Some human-derived drug-resistant transgenes are available for use in hematopoietic cells (37, 38), but they typically incorporate amino acid changes from the native protein sequence that may compromise their inability to remain nonimmunogenic and the continued presence of chemoselective drugs may slow kinetics of *ex vivo* numerical expansion and alter T-cell function.

Coupling electrotransfer of *SB* system with selective propagation of CAR^+ T cells was made possible using K562 cells that had been

genetically modified to express costimulatory molecules to function as aAPC. We have previously shown that the presence of 4-1BBL and MICA on $CD19^+$ K562 could propagate $CD19R^+$ T cells (18). However, sustained antigen-driven numerical expansion of genetically modified T cells on aAPC has required the presence of rhIL-15 (18). In our current experiments, we found that the exogenous addition of this soluble cytokine led to nonspecific stimulation of T cells after electrotransfer, especially because there was no concomitant drug selection, resulting in the outgrowth of T cells that did not maintain CAR expression (data not shown). This could be corrected by expression of IL-15 at the interface between aAPC and T cells, using membrane-bound IL-15, as has been shown for the survival/propagation of NK cells (19, 39). This approach of expressing IL-15 on the cell surface has the further advantage of avoiding rhIL-15 protein that is not yet readily/widely available for use in clinical trials. Allogeneic LCL are another source of $CD19^+$ aAPC to propagate CD19-specific T cells and are available to many centers operating facilities in compliance with cGMP as a master cell bank. However, the presence of HLA led to stimulation of T cells through activation of allospecific TCR and subsequent outgrowth of T cells that lacked CAR expression. This alloimmune response could be avoided using the K562 as aAPC, as these cells lack endogenous class I and II MHC (29).

Next-generation clinical trials using genetically modified T cells are expected to infuse predefined populations of T cells with defined characteristics such as the inclusion of both $CD4^+$ and $CD8^+$ T cells and T_{CM}. There is convincing clinical data that the presence of $CD4^+$ T-helper cells improves the persistence of $CD8^+$ antigen-specific T cells (40). Furthermore, clinical trials using melanoma-specific T cells have shown *in vivo* long-term persistence of subpopulations of infused $CD28^+$ memory T cells (41) and human experience has shown a preference for the selective survival of autologous HIV-specific $CD27^+$ versus $CD27^{neg}$ adoptively transferred T cells (31). These data are supported by nonhuman experiments in which adoptive transfer of *ex vivo* propagated macaque $CD28^+CD95^+CD62L^+$ T_{CM} resulted in longer *in vivo* persistence compared with infusion of numerically expanded effector T cells (34). We note that the electrotransfer of *SB* plasmids and subsequent CAR-mediated propagation on aAPC supports the outgrowth of T cells with these desired phenotypes as our CAR^+ T cells maintain expression of CD27, CD28, CD45RO, CD95, and CD62L. Clinical trials will be needed to determine whether adoptive transfer of these CAR^+ T cells with an apparent central memory immunophenotype ($CD28^+CD95^+CD62L^+$) results in long-term *in vivo* persistence of genetically modified T cells or whether these cells, despite being maintained for weeks in culture, will differentiate after infusion into effector T cells with limited *in vivo* survival. Clinical experience will also be needed to assess whether the presence of CD62L (L-selectin) on genetically modified T cells enables CAR^+ T cells to traffic to sites of minimal residual disease for B-lineage malignancies, such as secondary lymphoid organs (42, 43).

Although there are a variety of transposase/transposon expression vectors available, we elected to combine the improved enzymatic activity of the SB11 transposase with pT IR sequences, rather than less efficient SB10 transposase with pT2 plasmid containing IR with improved IR activity. This was based on (*a*) the observation that integrated SB11 transposase could not be detected after T-cell culture on aAPC and (*b*) the assumption that because the CAR transposon with flanking IR is to be integrated, we wished to reduce the potential for introducing an element with increased potential for retransposition and potential deleterious chromosomal rearrangement. We note that the majority of viral vectors currently used in human gene therapy trials also contain elements flanking transgene to be integrated, such as the long terminal repeat (LTR) termini of recombinant retrovirus, with binding sites for enzymes with integrase activity. The transfer of retroviral-derived LTR has not been associated with deleterious host genome chromosome rearrangements, especially in T cells (44), and the low risk of genotoxicity due to the integrated presence of *SB* IR should be on par with retrovirally mediated transduction.

A gene transfer event with stable integration could result in deleterious insertional mutagenesis, but for *SB* transposition this seems to be less than retrovirally mediated transduction given the observed preference for random chromosomal integration at TA-dinucleotide base pairs areas. Although the safety of *SB* transposition can only be adequately addressed in clinical trials, we have not seen major chromosomal aberrations after electrotransfer of *SB* plasmids. Furthermore, to safeguard against the emergence of genetically modified T cells with autonomous growth, we routinely culture T cells after electroporation without aAPC and we are yet to observe evidence of antigen-independent proliferation. The risks for first-in-human trials using *SB* system would seem to be ameliorated when using T cells, rather than hematopoietic progenitor cells and in the setting of high-risk malignancies in which patients are expected to succumb to underlying relapsed malignancies. The risks of genotoxicity may be reduced in the future using a transposase with directed integration (45, 46), coupling persistent transposase activity with a transgene mediating conditional suicide, or introducing mRNA (47) rather than DNA coding for the transposase.

The future for clinical therapy infusing genetically modified T cells with redirected specificity looks promising. There are published reports on the therapeutic effect of T cells genetically modified to express full-length $\alpha\beta$TCR (48) and clinical studies using T cells expressing chimeric receptors to redirect specificity have been reported or are under way (35, 49, 50). With the results of the first in-human trial infusing CD19-specific T cells being reported (3), the next step (the so-called second translational hurdle) will be expanding these single-institution experiences to multi-institution trials powered for efficacy. The platform we describe for producing CAR^+ T cells should be appealing to investigators undertaking single-site as well as multisite trials using gene transfer of immunoreceptor(s) to redirect the specificity of T cells, including T_{CM}. The system we have developed uses technology that is readily accessible and practiced in compliance with cGMP for phase I/II trials because we use (*a*) DNA plasmids, (*b*) electroporation using a commercial device, (*c*) weekly addition of irradiated immortalized aAPC feeder cells derived from K562 (which are available for use in cGMP), and (*d*) addition of exogenous rhIL-2 purchased through pharmacy stores.

In conclusion, we report a new gene transfer approach for the clinical application of T cells with redirected specificity for desired antigens. It is anticipated that this approach will be of interest not just for generating clinical grade T cells with specificity for CD19, but for genetically modifying T cells to express CAR with alternative specificities as well as for introducing TCR transgenes. Most adoptive immunotherapy trials that have shown therapeutic efficacy, e.g., to melanoma, CMV, EBV, and adenoviral antigens, have all used an *in vitro* antigen-driven proliferation step to propagate antigen-specific T cells before infusion. We have now incorporated *ex vivo*

CAR-dependent proliferation to derive genetically modified T cells and will evaluate the CD19-specific T cells, using *SB* transposition and aAPC, in a next-generation clinical trial.

Acknowledgments

Received 9/21/2007; revised 12/19/2007; accepted 1/17/2008.

Grant support: Cancer Center Core Grant CA16672; RO1 CA124782 and CA120956; R21 CA129390 and CA116127; Department of Defense grant PR064229; The Alliance for Cancer Gene Therapy; The Alex's Lemonade Stand Foundation; The Carl C. Anderson, Sr. and Marie Jo Anderson Charitable Foundation; The Gillson Longenbaugh Foundation; The J.P. McCarthy Fund Developmental Grant Program; The Leukemia and Lymphoma Society; The Lymphoma Research Foundation; The Miller Foundation, The National Foundation for Cancer Research; The National Marrow Donor Program; and The Pediatric Cancer Research Foundation.

The costs of publication of this article were defrayed in part by the payment of page charges. This article must therefore be hereby marked *advertisement* in accordance with 18 U.S.C. Section 1734 solely to indicate this fact.

We thank Dr. Mark Kay at Stanford School of Medicine, Stanford, CA, for providing the pT plasmid; Dr. John Rossi at City of Hope Cancer Center, Duarte, CA, for his valuable suggestions; Karen Ramirez and David He from Flow Cytometry Core Laboratory (NIH grant 5P30CA016672-32) for their help with flow cytometry; Jim Wygant and Dr. Brad McIntrye in the Immunology Core for their help with the monoclonal antibody production; and Dr. Asha Multani from T.C. Hsu Molecular Cytogenetics Core for her assistance with G-banding.

References

1. Cooper LJ, Topp MS, Serrano LM, et al. T-cell clones can be rendered specific for CD19: toward the selective augmentation of the graft-versus-B-lineage leukemia effect. Blood 2003;101:1637–44.
2. Serrano LM, Pfeiffer T, Olivares S, et al. Differentiation of naive cord-blood T cells into CD19-specific cytolytic effectors for posttransplantation adoptive immunotherapy. Blood 2006;107:2643–52.
3. Jensen MC, Popplewell L, DiGiusto DL, et al. A first-n-human clinical trial of adoptive therapy using CD19-specific chimeric antigen receptor re-directed T cells for recurrent/refractory follicular lymphoma. Mol Ther 2007;15:S142.
4. Lupton SD, Brunton LL, Kalberg VA, Overell RW. Dominant positive and negative selection using a hygromycin phosphotransferase-thymidine kinase fusion gene. Mol Cell Biol 1991;11:3374–8.
5. Kowolik CM, Topp MS, Gonzalez S, et al. CD28 costimulation provided through a CD19-specific chimeric antigen receptor enhances *in vivo* persistence and antitumor efficacy of adoptively transferred T cells. Cancer Res 2006;66:10995–1004.
6. Cid-Arregui A, Juarez V, zur Hausen H. A synthetic E7 gene of human papillomavirus type 16 that yields enhanced expression of the protein in mammalian cells and is useful for DNA immunization studies. J Virol 2003;77:4928–37.
7. Patterson SS, Dionisi HM, Gupta RK, Sayler GS. Codon optimization of bacterial luciferase (lux) for expression in mammalian cells. J Ind Microbiol Biotechnol 2005;32:115–23.
8. Berger C, Huang ML, Gough M, Greenberg PD, Riddell SR, Kiem HP. Nonmyeloablative immunosuppressive regimen prolongs *in vivo* persistence of gene-modified autologous T cells in a nonhuman primate model. J Virol 2001;75:799–808.
9. Jung D, Jaeger E, Cayeux S, et al. Strong immunogenic potential of a B7 retroviral expression vector: generation of HLA-B7-restricted CTL response against selectable marker genes. Hum Gene Ther 1998;9:53–62.
10. Ivics Z, Hackett PB, Plasterk RH, Izsvak Z. Molecular reconstruction of Sleeping Beauty, a Tc1-like transposon from fish, and its transposition in human cells. Cell 1997;91:501–10.
11. Izsvak Z, Ivics Z. Sleeping beauty transposition: biology and applications for molecular therapy. Mol Ther 2004;9:147–56.
12. Geurts AM, Hackett CS, Bell JB, et al. Structure-based prediction of insertion-site preferences of transposons into chromosomes. Nucleic Acids Res 2006;34:2803–11.
13. Huang X, Wilber AC, Bao L, et al. Stable gene transfer and expression in human primary T cells by the Sleeping Beauty transposon system. Blood 2006;107:483–91.
14. Robbin PB, Yu XJ, Skelton DM, et al. Increased probability of expression from modified retroviral vectors in embryonal stem cells and embryonal carcinoma cells. J Virol 1997;71:9466–74.
15. Holli RP, Nightingal SJ, Wan X, et al. Stable gene transfer to human CD34(+) hematopoietic cells using the Sleeping Beauty transposon. Exp Hematol 2006;34:1333–43.
16. Yan SR, Meus L, Chi W, Ivic Z, Izsva Z, Ka MA. Somatic integration and long-term transgene expression in normal and haemophilic mice using a DNA transposon system. Nat Genet 2000;25:35–41.
17. Geurts AM, Yang Y, Clar KJ, et al. Gene transfer into genomes of human cells by the sleeping beauty transposon system. Mol Ther 2003;8:108–17.
18. Numbenjapon T, Serrano LM, Singh H, et al. Characterization of an artificial antigen-presenting cell to propagate cytolytic CD19-specific T cells. Leukemia 2006;20:1889–92.
19. Imai C, Iwamoto S, Campana D. Genetic modification of primary natural killer cells overcomes inhibitory signals and induces specific killing of leukemic cells. Blood 2005;106:376–83.
20. Cooper LJ, Al-Kadhimi Z, Serrano LM, et al. Enhanced antilymphoma efficacy of CD19-redirected influenza MP1-specific CTLs by cotransfer of T cells modified to present influenza MP1. Blood 2005;105:1622–31.
21. Pathak S. Chromosome banding techniques. J Reprod Med 1976;17:25–8.
22. Scholten KB, Kramer D, Kueter EW, et al. Codon modification of T cell receptors allows enhanced functional expression in transgenic human T cells. Clin Immunol 2006;119:135–45.
23. Cooper LJ, Ausubel L, Gutierrez M, et al. Manufacturing of gene-modified cytotoxic T lymphocytes for autologous cellular therapy for lymphoma. Cytotherapy 2006;8:105–17.
24. Jensen MC, Clarke P, Tan G, et al. Human T lymphocyte genetic modification with naked DNA. Mol Ther 2000;1:49–55.
25. Riddell SR, Greenberg PD. The use of anti-CD3 and anti-CD28 monoclonal antibodies to clone and expand human antigen-specific T cells. J Immunol Methods 1990;128:189–201.
26. Gresch O, Engel FB, Nesic D, et al. New non-viral method for gene transfer into primary cells. Methods 2004;33:151–63.
27. Cui Z, Geurts AM, Liu G, Kaufman CD, Hackett PB. Structure-function analysis of the inverted terminal repeats of the sleeping beauty transposon. J Mol Biol 2002;318:1221–35.
28. Butler MO, Lee JS, Ansen S, et al. Long-lived antitumor CD8+ lymphocytes for adoptive therapy generated using an artificial antigen-presenting cell. Clin Cancer Res 2007;13:1857–67.
29. Suhoski MM, Golovina TN, Aqui NA, et al. Engineering artificial antigen-presenting cells to express a diverse array of co-stimulatory molecules. Mol Ther 2007;15:981–8.
30. Bachmann MF, Wolint P, Schwarz K, Jager P, Oxenius A. Functional properties and lineage relationship of $CD8^+$ T cell subsets identified by expression of IL-7 receptor α and CD62L. J Immunol 2005;175:4686–96.
31. Ochsenbein AF, Riddell SR, Brown M, et al. CD27 expression promotes long-term survival of functional effector-memory $CD8^+$ cytotoxic T lymphocytes in HIV-infected patients. J Exp Med 2004;200:1407–17.
32. Sallusto F, Lenig D, Forster R, Lipp M, Lanzavecchia A. Two subsets of memory T lymphocytes with distinct homing potentials and effector functions. Nature 1999;401:708–12.
33. Baron V, Bouneaud C, Cumano A, et al. The repertoires of circulating human CD8(+) central and effector memory T cell subsets are largely distinct. Immunity 2003;18:193–204.
34. Berger C, Jensen MC, Lansdorp PM, Gough M, Elliott C, Riddell SR. Adoptive transfer of effector CD8 T cells derived from central memory cells establishes persistent T cell memory in primates. J Clin Invest 2008;118:294–305.
35. Park JR, Digiusto DL, Slovak M, et al. Adoptive transfer of chimeric antigen receptor re-directed cytolytic T lymphocyte clones in patients with neuroblastoma. Mol Ther 2007;15:825–33.
36. Bell JB, Aronvovich EL, Schriefels JM, Clifford AM, Hoekstra ND, Whitley CB, Hackett PB. Duration of expression of Sleeping Beauty transposase in mouse liver following hydrodynamic delivery. Mol Ther 2006;13 Suppl 1:S150.
37. Sato T, Neschadim A, Konrad M, Fowler DH, Lavie A, Medin JA. Engineered human tmpk/AZT as a novel enzyme/prodrug axis for suicide gene therapy. Mol Ther 2007;15:962–70.
38. Yam P, Jensen M, Akkina R, et al. *Ex vivo* selection and expansion of cells based on expression of a mutated inosine monophosphate dehydrogenase 2 after HIV vector transduction: effects on lymphocytes, monocytes, and $CD34^+$ stem cells. Mol Ther 2006;14:236–44.
39. Wittnebel S, Da Rocha S, Giron-Michel J, et al. Membrane-bound interleukin (IL)-15 on renal tumor cells rescues natural killer cells from IL-2 starvation-induced apoptosis. Cancer Res 2007;67:5594–9.
40. Rooney CM, Smith CA, Ng CY, et al. Infusion of cytotoxic T cells for the prevention and treatment of Epstein-Barr virus-induced lymphoma in allogeneic transplant recipients. Blood 1998;92:1549–55.
41. Powell DJ, Jr., Dudley ME, Robbins PF, Rosenberg SA. Transition of late-stage effector T cells to $CD27^+$ $CD28^+$ tumor-reactive effector memory T cells in humans after adoptive cell transfer therapy. Blood 2005;105:241–50.
42. Galkina E, Florey O, Zarbock A, et al. T lymphocyte rolling and recruitment into peripheral lymph nodes is regulated by a saturable density of L-selectin (CD62L). Eur J Immunol 2007;37:1243–53.
43. Mitoma J, Bao X, Petryanik B, et al. Critical functions of N-glycans in L-selectin-mediated lymphocyte homing and recruitment. Nat Immunol 2007;8:409–18.
44. Bonini C, Bondanza A, Perna SK, et al. The suicide gene therapy challenge: how to improve a successful gene therapy approach. Mol Ther 2007;15:1248–52.
45. Ivics Z, Katzer A, Stuwe EE, Fiedler D, Knespel S, Izsvak Z. Targeted sleeping beauty transposition in human cells. Mol Ther 2007;15:1137–44.
46. Yant SR, Huang Y, Akache B, Kay MA. Site-directed transposon integration in human cells. Nucleic Acids Res 2007;35:e50.
47. Wilber A, Wangensteen KJ, Chen Y, et al. Messenger RNA as a source of transposase for Sleeping Beauty transposon-mediated correction of hereditary tyrosinemia type I. Mol Ther 2007;15:1280–7.
48. Morgan RA, Dudley ME, Wunderlich JR, et al. Cancer regression in patients after transfer of genetically engineered lymphocytes. Science 2006;314:126–9.
49. Kershaw MH, Westwood JA, Parker LL, et al. A phase I study on adoptive immunotherapy using gene-modified T cells for ovarian cancer. Clin Cancer Res 2006;12:6106–15.
50. Lamers CH, Langeveld SC, Groot-van Ruijven CM, Debets R, Sleijfer S, Gratama JW. Gene-modified T cells for adoptive immunotherapy of renal cell cancer maintain transgene-specific immune functions *in vivo*. Cancer Immunol Immunother 2007;56:1875–83.